Concrete Bridge Deck Deterioration Assessment Using Ground Penetrating Radar

Research Final Report from the University of Tennessee, Knoxville | Da Hu, Shuai Li, Z. John Ma, Baoshan Huang | May 31, 2021

DISCLAIMER

This research was funded through the State Planning and Research (SPR) Program by the Tennessee Department of Transportation and the Federal Highway Administration under ***RES 2019-17: Concrete Bridge Deck Deterioration Assessment Using Ground Penetrating Radar.***

This document is disseminated under the sponsorship of the Tennessee Department of Transportation and the United States Department of Transportation in the interest of information exchange. The State of Tennessee and the United States Government assume no liability of its contents or use thereof.

The contents of this report reflect the views of the author(s) who are solely responsible for the facts and accuracy of the material presented. The contents do not necessarily reflect the official views of the Tennessee Department of Transportation or the United States Department of Transportation.

Technical Report Documentation Page

1. Report No. RES 2019-17	2. Government Accession No.	3. Recipient's Catalog No.
4. Title and Subtitle *Concrete Bridge Deck Deterioration Assessment Using Ground Penetrating Radar*		5. Report Date May 2021
		6. Performing Organization Code
7. Author(s) Da Hu, Shuai Li, Z. John Ma, Baoshan Huang		8. Performing Organization Report No.
9. Performing Organization Name and Address Department of Civil and Environmental Engineering The University of Tennessee, Knoxville 325 John D. Tickle Engineering Building 851 Neyland Drive Knoxville, TN, 37996		10. Work Unit No. (TRAIS)
		11. Contract or Grant No. RES 2019-17
12. Sponsoring Agency Name and Address Tennessee Department of Transportation 505 Deaderick Street, Suite 900 Nashville, TN 37243		13. Type of Report and Period Covered Final report January 2019 – May 2021
		14. Sponsoring Agency Code
15. Supplementary Notes Conducted in cooperation with the U.S. Department of Transportation, Federal Highway Administration.		

16. Abstract

Ground penetrating radar (GPR) is a non-destructive technique that has been used to inspect and assess concrete bridge deck deterioration. The objective of this project is to investigate the use of GPR in concrete bridge deck inspection and develop semi-automated tools to process GPR data for detecting, mapping, and visualizing potential deterioration areas of bridge decks. In this study, appropriate GPR system configuration and scanning parameters were discussed and identified to achieve efficient collection of GPR data suitable for bridge deck inspection. The GPR scans containing signatures resulted from different defects were investigated to examine the potential of GPR in bridge deck inspection.

A workflow and semi-automated data processing methods were developed in this study to generate bridge deck deterioration maps from collected GPR scans. First, the random forest model was trained to detect regions in a GPR scan containing hyperbolic signatures reflected from rebars in a bridge deck. Then, a robust hyperbola fitting method was used to fit each hyperbolic signature in the rebar region to locate the rebar. Thereafter, the estimated rebar locations and corresponding depth-corrected amplitudes were extracted to detect potential deterioration areas. Color-coded maps were automatically generated to visually represent potential deterioration areas of concrete bridge decks, which could assist subsequent inspection and maintenance. The developed GPR-based bridge deck inspection workflow and methods were tested in three case studies of bridge deck survey. The workflow and tools could help expedite GPR data collection and processing for bridge deck assessment.

17. Key Words **Ground penetrating radar, Bridge Deck Assessment, Deterioration, Machine Learning**		18. Distribution Statement No restriction. This document is available to the public from the sponsoring agency at the website http://www.tn.gov/	
19. Security Classif. (of this report) Unclassified	20. Security Classif. (of this page) Unclassified	21. No. of Pages 48	22. Price

Acknowledgement

This project partially supported the publication of two conference papers:

Executive Summary

The purpose of this study was to investigate the use of ground penetrating radar (GPR) in concrete bridge deck inspection, and develop semi-automated tools to process GPR data for detecting, mapping, and visualizing potential deterioration areas of bridge decks, which may facilitate the adoption of GPR for bridge inspection and asset management. Bridges are critical infrastructure systems to support transportation. There are about 20,000 highway bridges in the state of Tennessee that need to be inspected periodically to ensure safety and plan possible maintenance and repair. Traditional methods for concrete bridge deck condition assessment such as visual inspection, chain dragging, and hammer sounding are subjective and time-consuming. GPR is a non-destructive testing technique that can complement these traditional methods to provide quantitative data for bridge deck inspection and condition assessment. For the Tennessee Department of Transportation (TDOT) to adopt GPR for bridge inspection and assessment, critical issues need to be investigated to assess the practical applicability of GPR for concrete bridge deck deterioration assessment. First, the lack of understanding of appropriate GPR system configurations and scanning parameters results in inefficient operations of GPR system for bridge data acquisition. As such, bridge inspectors may waste time and efforts collecting low-quality data that are not appropriate for deterioration assessment. Second, GPR scans are not intuitive for interpretation, and GPR data processing is predominantly manual, hindering the use of GPR in bridge deck assessment at a large scale. In addition, the bridge deck information, such as the potential deterioration areas extracted from GPR scans, is not presented in an easy-to-understand manner, preventing detailed inspection, data inventory, reporting, and maintenance. These critical issues need to be addressed before TDOT can adopt GPR to inspect and assess the concrete bridge decks.

To address the critical need, two research objectives were pursued. The first objective was to identify appropriate GPR system configurations and parameters to achieve efficient and effective bridge data collection. In addition, GPR scans of common defects collected from computer simulations and laboratory experiments were analyzed to explore the potential of GPR in bridge inspection. The second objective was to develop a workflow and associated tools for processing GPR data and produce deterioration maps of bridge decks. A machine-learning based method was developed to detect rebars in a bridge deck, and the GPR signal amplitudes were used to detect potential deterioration areas. The deterioration information extracted from GPR scans can be visualized in two-dimensional (2D) color-coded maps to assist subsequent inspection and maintenance. Case studies were conducted to test the workflow and the developed tools. The key findings and recommendations derived from this study will help expedite the use of GPR for concrete bridge deck inspection and evaluation, and reduce the tedious efforts in extracting, visualizing, and documenting bridge deck deterioration information from non-intuitive GPR scans.

Key Findings

- GPR system configurations and scanning parameters will impact GPR data collection efficiency and data quality. Based on the review of literature and practice, for concrete bridge deck inspection, GPR system with antenna frequency from 1.5 GHz to 2.6 GHz should be used. Scanning with the following parameters may produce good quality data

in an efficient manner: 6-10 nanosecond (ns) time window, 512 samples per scan, 79 scans per meter, and 0.3-0.6m scan spacing. Scanning direction should be maintained perpendicular to the top rebar mat as much as possible.

- Using computer simulations and laboratory experiments, signal patterns of different bridge deck defects were investigated. It was found that rebar corrosion and concrete deterioration exhibit attenuated signal amplitudes or blurry hyperbolic features at rebar locations, which can be used to indicate potential deterioration areas. Delamination that has a thickness greater than 1mm developed at shallow depth in the bridge deck exhibits signatures in GPR scans. Delamination with a thickness smaller than 0.3mm in the bridge deck does not present noticeable signatures in the collected GPR scans, and thus is difficult to be detected.

- Detecting and locating rebars in GPR scans, and assessing the signal amplitude attenuation are critical steps to process GPR data to indicate the areas of potential deterioration in concrete bridge decks. A machine learning method based on random forest classification and robust hyperbola fitting was developed to locate the rebar and extract the amplitudes for deterioration assessment.

- After signal amplitude normalization and depth correction, median absolute deviation can be used to set the threshold value to detect potential deterioration areas. Color-coded maps can visually represent and quantitatively estimate the bridge deck deterioration areas. The proposed methods and workflow were tested in case studies, confirming the potential of using GPR for concrete bridge deck inspection and assessment.

Key Recommendations

GPR can be used as a complementing technique to existing methods for concrete bridge deck deterioration assessment. To expedite the use of GPR in bridge deck assessment, appropriate system configurations and scanning parameters should be used to ensure data collection efficiency, and automated processing methods should be used to reduce the efforts in manual analysis and interpretation. Estimating and visualizing potential deterioration areas of bridge deck from GPR scans should be implemented to provide quantitative information for inspection, asset management, and decision-making. GPR results should be carefully examined and interpreted when used for detecting and characterizing specific defects such as delamination. For complete and more accurate bridge deck deterioration assessment, GPR can be used in conjunction with other methods to improve the assessment performance.

Table of Contents

List of Tables

List of Figures

Chapter 1   Introduction

1.1 Problem Statement

Bridges are critical infrastructure systems that are essential for fulfilling transportation needs and maintaining societal functions. In Tennessee, there are 953 structurally deficient bridges, which are 4.7 percent of all bridges in Tennessee [1]. In addition, the state estimated that 7,257 bridges are in need of repairs and it would cost $8.3 billion to fix them [1]. Traditional methods for concrete bridge deck condition assessment such as visual inspection, chain dragging, and hammer sounding are subjective, expensive, time-consuming, and error-prone [2]. Ground penetrating radar (GPR) is a nondestructive testing technology that can rapidly provide quantitative data of concrete bridge decks for deterioration assessment. For the Tennessee Department of Transportation (TDOT) to adopt GPR for bridge inspection and assessment, critical issues need to be investigated to assess the practical applicability of GPR for concrete bridge deck deterioration assessment. First, the lack of understanding of appropriate GPR system configurations and scanning parameters results in inefficient operations of GPR system for bridge data acquisition. As such, bridge inspectors may waste time and efforts collecting low-quality data that are not appropriate for deterioration assessment. Second, GPR scans are not intuitive for interpretation, and GPR data processing is predominantly manual. Many person-hours are needed from professionals with extensive experience in GPR data processing to recognize defects and locate deterioration areas. The lack of semi-automated data processing tools hinders the use of GPR in bridge deck assessment at a large scale. In addition, the bridge deck information, such as the potential deterioration areas extracted from GPR scans, is not presented in an easy-to-understand manner, preventing detailed inspection, data inventory, reporting, and maintenance. These critical issues need to be addressed before TDOT can adopt GPR to inspect and assess the concrete bridge decks.

1.2 Objective

The goal of this project is to investigate the use of GPR in concrete bridge deck inspection, and develop semi-automated tools to process GPR data for detecting, mapping, and visualizing potential deterioration areas of a bridge deck, which may facilitate the adoption of GPR at TDOT for bridge inspection and asset management. To this end, there are two objectives.

- The first objective is to identify appropriate GPR system configurations and parameters for bridge data collection, including global positioning system (GPS) integration, antenna frequency, number of scans per unit of distance, range, number of samples per scan, transmit rate, traverse spacing, and scanning direction. In addition, GPR scans of common defects collected from computer simulations and laboratory experiments were analyzed to explore the potential of GPR in bridge inspection.

- The second objective is to develop a workflow and associated tools for processing GPR data and produce deterioration maps of bridge decks. A machine-learning based method was developed to detect rebars in a bridge deck, and the GPR signal amplitudes were used to detect potential deterioration areas. The deterioration information extracted from GPR scans can be visualized in two-dimensional (2D) maps to assist subsequent inspection and maintenance. Case studies were conducted to test the workflow and the

developed tools.

1.3 Method Overview

- Relevant GPR studies and current practice were reviewed to examine and identify appropriate GPR system configurations and parameters suitable for concrete bridge deck survey and inspection. The suggested configuration and parameters were used in case studies for bridge survey and inspection.

- Computer simulations were performed to generate GPR scans of bridge defects. Experiments were conducted to collect real GPR scans on concrete decks made with artificial defects. The GPR scans were used to investigate the signal patterns and features of defects to examine the potential of using GPR to detect and characterize bridge deck defects and deterioration areas.

- Concrete deterioration and rebar corrosion may lead to weak rebar reflection amplitudes in GPR scans. Potential deterioration areas in a bridge deck can be detected and mapped by analyzing the GPR signal amplitudes at the rebar locations. A workflow and machine-learning based data processing tools were developed to detect, map, and visualize potential deterioration areas of a bridge deck from collected GPR data. First, random forest model was trained to detect regions with hyperbolic signatures representing rebars in a GPR scan. Then, a robust hyperbola fitting method was used to fit the points extracted from the regions, and estimate the rebar locations. Thereafter, signal amplitudes at the rebar locations were extracted and processed to find the weak reflections that are indicative of deterioration areas. Finally, a color-coded map was generated to visually represent the deterioration areas, providing guidance for professionals for subsequent inspection and maintenance.

- Case studies were conducted to use the developed workflow and tools for processing the GPR data collected from three concrete bridge decks, which demonstrated the usability of the developed methods and tools.

1.4 Report Overview

The organization of this report is as follows. Chapter 2 introduces the GPR system and its application in concrete bridge deck inspection and deterioration assessment. Relevant studies on bridge deck assessment using GPR were also reviewed. In Chapter 3, GPR system configurations and appropriate parameters suitable for bridge data collection were reviewed and discussed. In addition, GPR data collected from numerical simulations and fabricated concrete slabs were analyzed to investigate the GPR signal pattern of bridge deck defects and to explore the potential of using GPR to detect and characterize bridge defects. Chapter 4 illustrates the methods developed for processing GPR data and mapping deterioration areas of a bridge deck. The results from case studies were also presented. Chapter 5 provides a summary of this study and discusses future work for bridge deck condition assessment.

Chapter 2 Background

2.1 GPR System

A GPR system typically consists of transmitting and receiving antennas, a control unit, a display unit, and a power unit. The control unit is the central processing unit to control all functions of a GPR system and coordinate the operation of different components. The GPR transmitting antenna can generate short-duration high-power radiofrequency (RF) pulses of energy that transmit into the ground. When the energy encounters buried objects with different permittivities, it will be reflected, refracted, or scattered back to the surface. The GPR receiving antenna receives reflected RF pulses from objects beneath the ground. The transmitting and receiving antennas are typically encapsulated in a box also known as a GPR antenna. GPR operating frequency generally varies from 15 to 3000MHz. A low-frequency antenna provides deep penetration but low resolution. A high-frequency antenna provides high resolution but can only be used for shallow probing. Table 1 shows the relationship between the center frequency of antenna and penetration depth [3].

TABLE I

GPR Center frequency vs penetration depth [3]

Center Frequency (MHz)	Depth of Penetration (m)	Typical Applications
1600	0.5	Concrete Evaluation
900	1	Concrete Evaluation, Void Detection
400	4	Utility, Engineering, Environmental, Void Detection
270	6	Utility, Engineering, Geotechnical
200	7	Geotechnical, Engineering, Environmental
100	20	Geotechnical, Environmental, Mining
16 - 80	35 - 50	Geotechnical

Two types of GPR antennas are commonly used in bridge deck surveys: ground-coupled and air-coupled. The air-coupled antenna can be mounted on a vehicle running at traffic speeds for fast scanning and reducing traffic interruptions. The spatial resolution of air-coupled GPR is typically smaller than that of ground-coupled GPR, which can only provide a rough estimate for subsurface deterioration conditions. In addition, air-coupled GPR produces more difficult data to analyze since it requires complex processing procedures, such as calibration and signal normalization, to mitigate the effects of signal amplitude variability caused by antenna height variation and ringing of surface reflection [4]. Compared to air-coupled GPR, ground-coupled antenna has a higher spatial resolution and greater signal-noise ratio. In this study, the ground-coupled antenna was used to conduct the bridge survey and inspection.

2.2 GPR Basic Principles

GPR is a non-destructive technique that has been used to assess the conditions of concrete bridge decks [5]. Previous studies have demonstrated the feasibility and applicability of GPR for bridge deck inspection [6]. Strong signal attenuations in a GPR scan may indicate the presence of potential deterioration. For instance, rebar corrosion may produce low-density rust around the rebar, and then generates expansive pressure on the surrounding concrete. The severe rebar corrosion will cause crack initiation and propagation around the rebar in concrete. The cracks filled with air or water may cause the scattering of signal energy and signal attenuation. Hence, strong signal attenuation can be used as an indicator for reinforcement concrete deterioration [7].

GPR sends electromagnetic (EM) waves in a cone-shaped pattern to the subsurface and records the wave reflected back to the surface [8]. The ratio of the amplitude of the reflected wave to the amplitude of an incident wave is calculated as a function of the dielectric constant on each side of the medium interface. The larger the dielectric constant contrast is, the stronger the reflected wave amplitude. For instance, the interface between steel reinforcement and concrete can lead to a high reflected amplitude due to a great dielectric contrast [9]. In addition, the speed of an EM wave varies when traveling through different materials. The wave velocity can be estimated by Eq. (1), where C is the speed of light (30 cm/ns), ε is the dielectric constant of the material. Table 2 presents typical values of dielectric constant and velocity for some materials [3].

$$v = \frac{C}{\sqrt{\varepsilon}} \tag{1}$$

TABLE II
Material dielectric constant and wave velocity [3]

Material	Dielectric constant	Velocity (cm/ns)
Air	1	30.0
Glacial ice	3.6	19.0
PVC	3	17.3
Asphalt	3 - 5	13.4 – 17.3
Concrete	4 - 11	9.0 -15.0
Granite	4 - 7	11.3 -15.0
Sandstone	6	12.2
Shale	5 - 15	7.7 -13.4
Freshwater	80	3.4
Saturated Sand	20 - 30	5.5-6.7
Steel	Infinite	0

The ratio of reflected amplitude to the incident amplitude between material 1 and material 2 can be calculated by Eq. (2), where ε_1 and ε_2 represent the dielectric constant for material 1 and material 2, respectively. The reflection coefficient can be either positive or negative, which is between $-1<R<1$. The magnitude of R determines how much of the incident wave is reflected.

If the difference of relative permittivities across the interface is large, most of the incident waves will be reflected.

$$R = \frac{\sqrt{\varepsilon_1} - \sqrt{\varepsilon_2}}{\sqrt{\varepsilon_1} + \sqrt{\varepsilon_2}} \qquad (2)$$

Rebars are reflected as hyperbolic features in a GPR scan as shown in Figure 2-2. The hyperbolic feature is generated as the GPR antenna sends energy in a conical shape to the subsurface. Therefore, two-way travel time of received rebar reflection decreases as the antenna approaches the rebar and increases after passing the rebar peak location. The rebar radius is defined as R. In Figure 2-1, the X-axis and Y-axis represent GPR moving distance and two-way travel time from electromagnetic (EM) wave emission to wave reception, respectively. The position relationship between x_i, x_0 and rebar center meets the Pythagorean theorem shown in Eq. (3), where r_i represents the distance from starting position x_i of the antenna to surface of the rebar r_0 is the perpendicular distance from rebar to the surface point x_0, which is also the shortest distance.
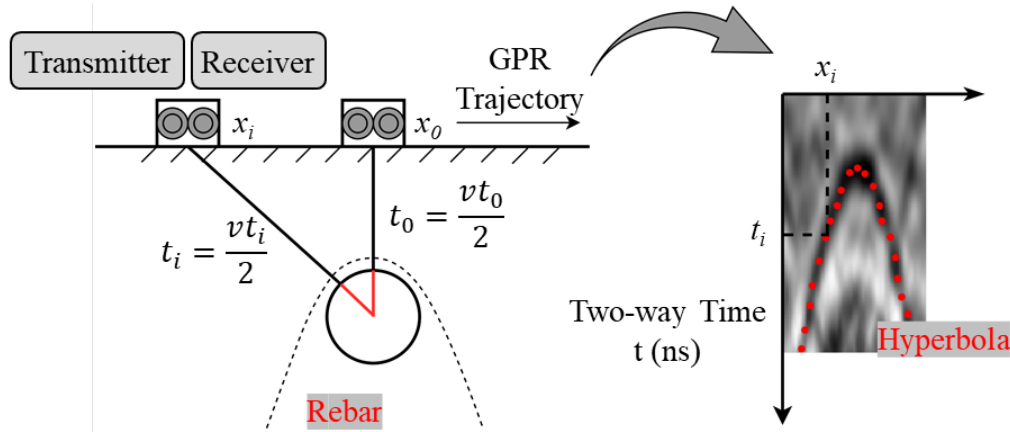
Figure 2-1. Mathematical Formulation of GPR reflection Generated by a Rebar

$$\left(r_i + R\right)^2 = \left(r_0 + R\right)^2 + \left(x_i - x_0\right)^2 \qquad (3)$$

Eq. (3) can be reformulated in Eq. (4), where v denotes the velocity of EM wave propagating in the concrete. The two-way travel times at location x_i and x_0 are expressed as t_i and t_0 in Eq. (4), respectively.

$$t_i = \frac{2}{v}\left[\sqrt{\left(\frac{vt_0}{2} + R\right)^2 + \left(x_i - x_0\right)^2} - R\right] \qquad (4)$$

Eq. (4) can then be rearranged to Eq. (5), which is a hyperbolic equation.

$$\frac{\left[t_i + \left(2R/v\right)\right]^2}{\left[t_0 + \left(2R/v\right)\right]^2} - \frac{\left(x_i - x_0\right)^2}{\left[\left(v/2\right)t_0 + R\right]^2} = 1 \qquad (5)$$

These hyperbolic signatures can be detected from a GPR scan to locate rebars in a bridge deck. The relative permittivity of rebar is significantly higher than concrete, therefore, most incident waves will be reflected back to the surface with a strong reflection amplitude recorded in GPR

data. The hyperbola peak represents the location of rebar, and its amplitude is an indicator of the bridge deck condition when rebar depth is constant throughout the bridge. The deteriorated concrete has a higher electrical conductivity compared to healthy concrete due to the presence of moisture and chloride ions [10]. A higher electrical conductivity leads to greater signal attenuation in the areas, which is shown as weaker rebar reflection amplitude in GPR scans [11]. Furthermore, cracks are common defects of concrete, which may be filled with air or water. The scattering of GPR signal energy will cause energy loss, and eventually lead to weak rebar reflection or blurry hyperbolic signatures. Therefore, weak rebar reflection and blurry hyperbola features can be used as indicators of bridge deck deterioration, such as concrete deterioration and/or corrosion of rebar. Figure 2-3 shows a GPR scan collected from a concrete bridge deck. As shown in the box, the hyperbolic signatures are not obvious in the GPR scan. Considering that rebars are typically equally spaced in the bridge deck and comparing with the regions with obvious hyperbolic signatures, the deterioration regions can be identified due to weak or blurry rebar signatures in the GPR scan.
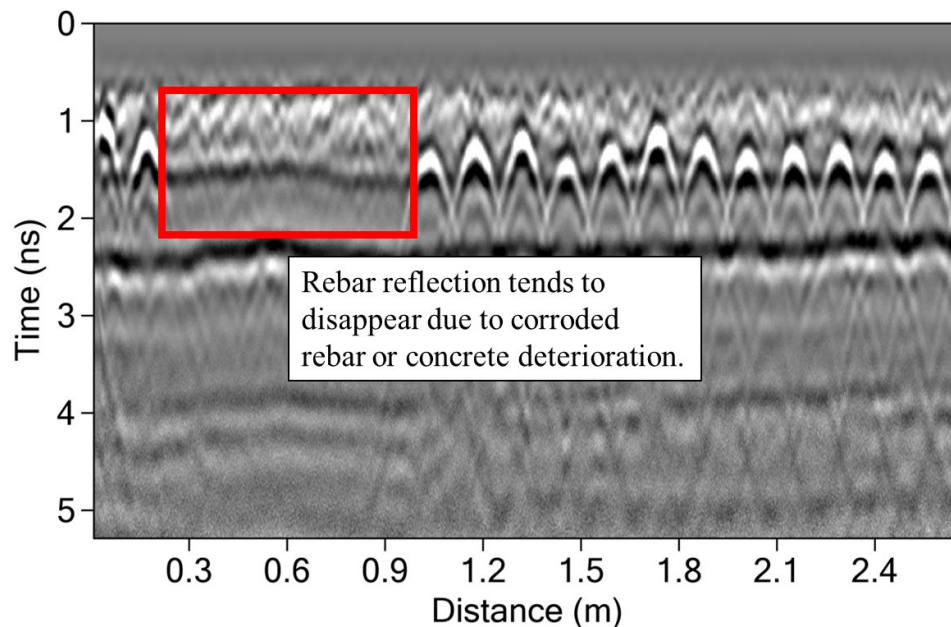
Figure 2-2. Example of GPR B-scan

2.3 GPR in Bridge Deck Condition Assessment

Detecting and locating deterioration areas is critical to timely and cost-effective bridge maintenance and rehabilitation. Using non-destructive testing techniques (NDT) for bridge deck inspection is cost-effective and less labor-intensive [2]. GPR is a NDT technique and has been demonstrated to be feasible and efficient in the assessment of bridge deck conditions [12]. For instance, Chung et al. [13] demonstrated the capability of GPR to detect deterioration areas such as debonding and scaling in asphalt-covered reinforced concrete bridge decks. The study also showed the potential of using GPR data to measure the thickness of asphalt and concrete cover over the rebar mat. In [14], air-coupled GPR was used to survey 92 bridge decks in Nova Scotia to find deterioration areas and estimate repair quantities. The area with potential deterioration is manually checked by comparing shape and travel time change of A-

scan waveform to GPR data from sound bridge deck. However, these methods are time-consuming and subjective, which is difficult to use in practice. To overcome these limitations, GPR B-scan has been used to assess bridge deck conditions. The GPR B-scan contains more information along the scanning direction and can eliminate amplitude anomalies during visual analysis caused by structural variation rather than corrosion [15].

More recently, image-based approaches have been used to detect bridge deck deterioration based on the fact that corroded rebars will cause signal attenuation [16]. The study analyzed the entire GPR profile with prior knowledge of structure characteristics to eliminate the effects of rebar depth, surface anomalies, and rebar spacing. However, this study requires prior knowledge of the structure and needs human interventions to process the data. Dinh et al. [17] proposed a convolutional neural network (CNN)-based method to detect and localize rebar from GPR B-scan. The method was integrated with conventional image processing techniques such as migration and thresholding. The results showed a very high detection accuracy, but CNN-based method always requires a lot of data to train the model. Rebar amplitudes were then extracted and processed to generate a deterioration map for the concrete bridge deck. In another study conducted by Dinh et al. [18], an automated rebar picking algorithm was proposed based on the Limited and Simplified Hyperbolic Summation technique. The performance of the method was sensitive to the hand-crafted threshold value.

In addition to the above studies, the reliability and efficiency of using GPR in bridge deck condition assessment have also been investigated. For instance, Dabous et al. [19] introduced a multi-sensor fusion method to integrate GPR and infrared thermography in bridge deck defects detection, and thus improving the reliability of detection results. In [20], the reliability of GPR for delamination detection in concrete was studied using the American Society for Testing and Materials (ASTM) procedure. The study concluded that the delamination detection solely based on GPR may lead to incorrect decisions, and the ability of GPR to image delamination is limited. The study by Varnavina et al. [21] suggested that the efficiency of GPR in estimating concrete deterioration quantities depends on the mapping of reinforcing steel. Furthermore, GPR has been demonstrated to be a promising method to complement visual inspection and other testing methods for evaluating bridge deck conditions [22].

Chapter 3   GPR Data Collection and Analysis

In this chapter, appropriate GPR system configurations and scanning parameters were reviewed and identified for bridge deck inspection and condition assessment. In addition, numerical simulations and laboratory experiments were conducted to examine the GPR signal patterns of bridge defects and to investigate the potential of using GPR for concrete bridge deck inspection and condition assessment.

3.1 GPR System Configuration and Parameters Settings

Table III reviews the GPR system and settings that have been used for concrete bridge deck assessment in related studies, including GPR antenna frequency, scanning spacing, samples per trace, and horizontal parameter. In addition to these parameters, time range, scanning direction, and GPS integration are also important configurations that are discussed as follows.

TABLE III
Summary of Relevant Studies

Source	Antenna frequency	Scanning spacing	Samples per trace	Horizontal parameter
Abouhamad et al. (2017) [16]	1.5 GHz	0.3m	N/A	N/A
Alani et al. (2013) [23]	2GHz	0.1m	N/A	N/A
Dinh et al. (2014) [24]	1.5 GHz	0.6m	512	N/A
Benedetto (2013) [25]	2GHz	N/A	N/A	N/A
Dabous et al. (2017) [19]	1.6 GHz	0.3m	N/A	N/A
Hasan and Yazdani (2014) [26]	1.6 GHz and 2.6 GHz	0.6m	512	92scans/s
Hugenschmidt (2002) [27]	1.2 GHz	N/A	N/A	N/A
Hugenschmidt and Mastrangelo (2006) [28]	1.2GHz	N/A	512	200;299 scans/m
Varnavina et al. (2015) [29]	1.5GHz	0.3; 0.6; 0.9; 1.2; 1.5; 1.8m	2048	79; 157; 236; 315; 394; 472 scans/m
Varnavina et al. (2017) [30]	1.5 GHz	0.3m	N/A	N/A
Wei and Zhang (2014) [31]	2.6 GHz	N/A	1024	N/A

Antenna frequency. The GPR antenna frequency used in bridge deck inspection typically ranges from 1.2GHz to 2.6GHz. The spatial resolution increases with the increase of the GPR antenna frequency. The typical thickness of a concrete bridge deck ranges from 17cm to 21cm, and the cover thickness of the top rebar mat is typically 5cm to 7cm [32]. The penetration depths for 1.2GHz and 2.6GHz are 76cm and 30cm, respectively. These penetration depths can fulfill the depth requirement for inspection given typical bridge deck thickness. The resolution of GPR antenna needs to be higher than the diameter of rebar, to ensure rebar features can

be recognized in the GPR data. The vertical resolutions for 1.2GHz and 2.6GHz are 6.1mm and 2.5mm, respectively [33]. Hence, GPR antenna in this range can detect rebar features in the GPR scans.

However, if there are cracks or delaminations in the bridge deck, low-frequency antennas like 1.2GHz may not be capable to detect them. Therefore, high-frequency antennas are preferred in the bridge deck condition assessment to enable more detailed analysis. For concrete bridge deck inspection, using the GPR with a 1.5GHz antenna or above is suggested.

Time range. Time range is the vertical scale in nanoseconds (ns) within which the GPR acquisition system will record reflections. A greater time range will allow EM waves to penetrate deeper into the ground and return deeper reflections. The time range is the two-way travel time, in other words, a range of 10ns recorded the deepest possible reflection is at 5ns. The selection of time range mainly depends on the depth of the target. A longer time range will slow the GPR data collection for that allotted time. In addition, the resolution of GPR data will be lowered with a longer time range if the number of samples is fixed. Therefore, it is important to select an appropriate time range to attain efficient GPR data collection and high-quality GPR data. For bridge deck, the thickness generally ranges from 17cm to 21cm. The relative permittivity of concrete typically varies from 4 to 11 [3]. As such, a time range of 5ns can reach the bottom of bridge deck. To ensure the GPR signal can penetrate from top to bottom of bridge deck, a time range of 6ns to 10ns is recommended, which can be further adjusted in the range based on the bridge deck thickness.

Scanning direction and spacing. Typically, GPR data are collected in the direction perpendicular to the top rebar orientation. Therefore, if the upper rebar orientation is longitudinal (i.e., direction of traffic), then GPR data should be collected perpendicular to the direction of traffic. The orientation of the top rebar mat can be simply determined by acquiring sample GPR data in both directions and then comparing the arrival times of the rebar reflections in the data. Note that, GPR scanning direction can only be approximately perpendicular to the top rebar mat in practice, because it is difficult to achieve a completely perpendicular scanning direction. The spacing of GPR scan is recommended to range from 0.3m to 0.6m depending on the time availability and bridge specification. For instance, a lower spacing in the range is recommended for a small bridge to ensure there is enough GPR data for subsequent analysis.

Vertical and horizontal parameters. The vertical parameter represents the number of samples per trace, which can affect data acquisition speed. According to GSSI [34], increasing the number of samples will increase computation cost and thus reducing data acquisition speed. The number of samples varies from 256 to 16384. The selection of samples per trace is related to the time range. If the time range is large, a small number of samples will lead to an aliasing issue. For the bridge deck, 512 samples per trace are recommended to achieve a high vertical resolution and maintain a high acquisition speed.

The horizontal parameter is the number of scans the system will collect per second for time-based data or per meter for distance-based data. In current practice, ground-coupled GPR mounted on the wheel cart is the most widely used data collection system. This configuration is generally set as distance-based mode. Reinforcing steel spacing typically varies from 15cm

to 30cm, which requires 79 scans per meter to be able to differentiate rebar signatures in GPR scan [30]. If the spacing is smaller than 15cm, a higher number of scans per meter may be needed.

GPS integration. The GPR scanning cart is equipped with an encoder wheel, which can measure distance along the moving direction. If the wheel cart moves along the straight parallel line, the inspector can match a specific location on the bridge deck with GPR scanning traces in B-scan based on distance information. However, if the GPR moves along the curve, it will be a challenge to accurately match them. Real-time Kinematic (RTK) GPS has been integrated with GPR to offer a more accurate positioning [35]. Good-quality GPS data allows distance corrections and is very helpful when GPR data are collected from wide areas without visual position referencing. GPS coordinates are typically associated with GPR scan numbers. A GPS coordinate file is recorded for every GPR B-scan during the survey. Therefore, every GPR B-scan is geo-registered and rebar locations on the bridge can be estimated.

Table IV summarizes appropriate GPR system scanning parameters. These parameters can expedite the GPR data collection process and ensure data quality for subsequent bridge deck condition assessment.

TABLE IV
Recommended GPR system scanning parameters

| Parameter	Recommendation
Antenna frequency	>= 1.5 GHz
GPS	Recommended
Time range	6-10ns
Samples per scan	512
Scans per meter	> 79
GPR scan spacing	0.3-0.6m
Scan direction	Perpendicular to top rebar

3.2 GPR Data Analysis

Numerical simulation and laboratory experiments were conducted to examine the signal pattern of bridge defects in GPR B-scan with appropriate parameters. Numerical simulation was adopted due to its flexibility and capability to simulate different defects in the bridge deck. GPR simulation was conducted by the finite-difference time-domain (FDTD) GPR modeling software called gprMax [36]. The research team examined four types of defects in bridge decks that are reinforced concrete deterioration, shallow delamination, intermediate delamination, and deep delamination. Table V presents the simulated defects and corresponding descriptions.

TABLE V
Common defects in concrete bridge decks

Defects	Definition
Reinforced concrete deterioration	Rust accumulates around the rebar due to exposure to a corrosive environment, and corrosion products cause crack initiation and propagation on surrounding concrete.
Shallow delamination	Cracks or fractures at or just above the level of top reinforcement.
Intermediate delamination	Cracks or fractures between the top and bottom reinforcement layer
Deep delamination	Cracks or fractures at or just below the level of bottom reinforcement.

Figure 3-1 shows the cross-section of an exemplary bridge deck design. The thickness of the bridge deck is 200mm. The rebar size is 13mm with 200mm spacing. The top rebar mat depth is 65mm and the bottom layer of reinforcement is 25mm from the bottom. This bridge deck design will serve as a reference for GPR simulation.
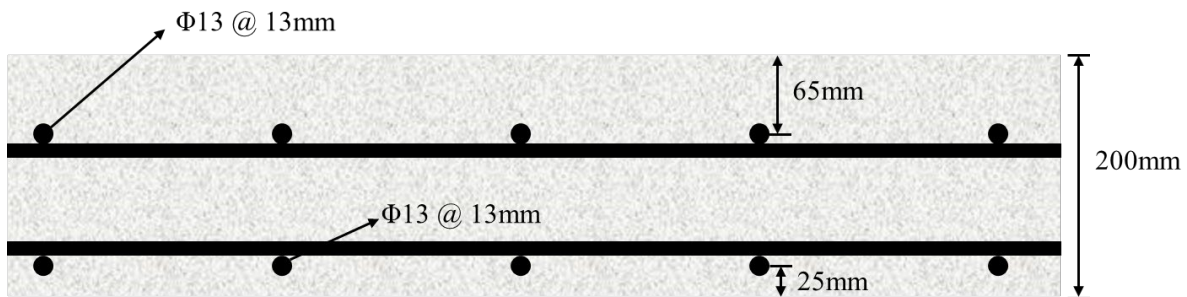
Figure 3-1. An Example of Bridge Deck Specification

The research team simulated GPR with a 2GHz antenna that is suitable for bridge deck inspection. Table VI presents the electromagnetic properties of materials used in the simulation.

TABLE VI
Material Electromagnetic Properties

Material	Dielectric Constant	Conductivity	Relative Permeability
Concrete [37]	7	0.001	1
Rebar	inf	inf	1
Air	1	0	1
Water [38]	80	4.1	1
Rust [38]	8.42	0.15	1

Table VII presents the simulated bridge deck and specification of simulated defects. Four different widths were simulated for shallow, intermediate, and deep delaminations that are 0.1mm, 0.3mm, 1mm, and 2mm. For reinforced concrete deterioration, the thickness of the rust layer is 2mm around the rebar. The maximum width of cracks extending from the rebar is approximately 0.3mm. The cracks fill with air and water scenarios were simulated, separately.

Note that, numerical simulation assumes that GPR scan is perpendicular to the top rebar mat and is between the two adjacent rebars of the second layer. This is because if the GPR scan is exactly on the top of the second rebar layer, GPR signal will not be able to penetrate through this reinforcement layer in the 2D simulation. To explore the feasibility of GPR in detecting intermittent and deep delamination, the cross-section of the simulated model only includes the two layers that are perpendicular to GPR scans.
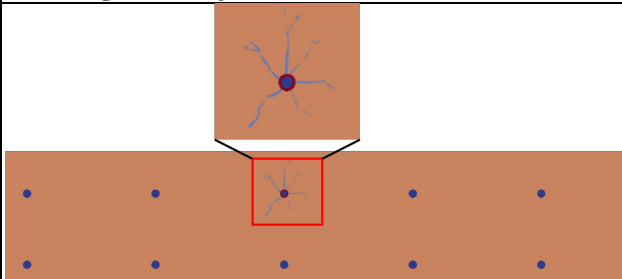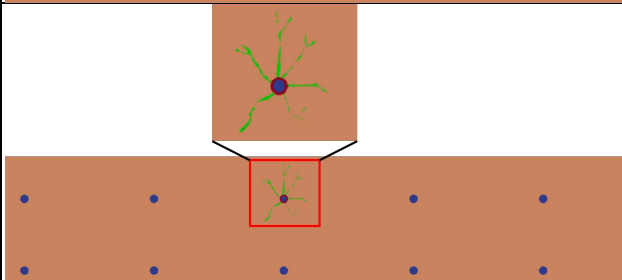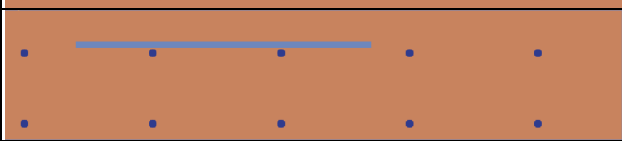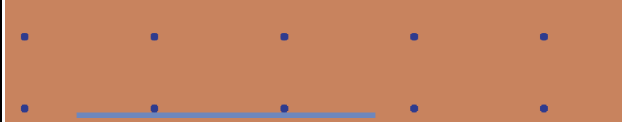
TABLE VII
Simulation Cases

Defects	Model geometry	Description
Reinforcement concrete deterioration (crack filled with air)		Corroded rebar with crack filled with air
Reinforcement concrete deterioration (crack filled with water)		Corroded rebar with crack filled with water
Shallow delamination		Width: 0.1mm, 0.3mm, 1mm, and 2mm
Intermediate delamination		Width: 0.1mm, 0.3mm, 1mm, and 2mm
Deep delamination		Width: 0.1mm, 0.3mm, 1mm, and 2mm

Figure 3-2 shows the GPR signatures for reinforcement concrete deterioration with cracks filled with air in the bridge deck. The simulated result indicates that rebar amplitude of deteriorated areas is smaller than that of healthy concrete. This is because the presence of cracks causes the scattering of GPR signals which leads to signal attenuation.
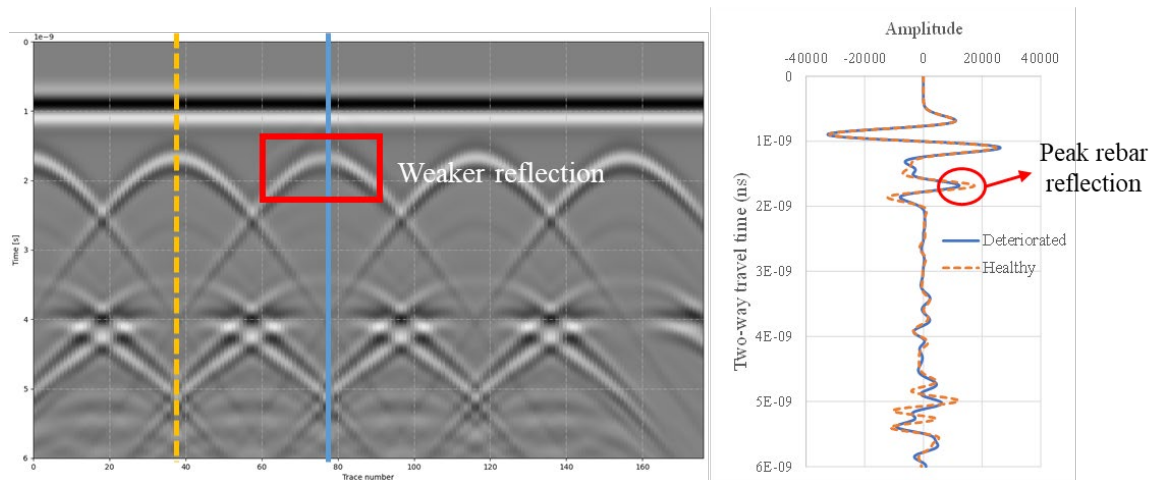
Figure 3-2. GPR Signatures of Reinforcement Concrete Deterioration with Cracks Filled with Air

Figure 3-3 presents GPR scans for reinforcement concrete deterioration with cracks filled with water in the bridge deck. The deterioration with water-filled cracks displays a clutter signal pattern at the rebar position. In addition, the hyperbola reflection of rebar is barely recognized in this area, which indicates that concrete has deteriorated. This is because that if the bridge deck is in good condition, there will be significant rebar reflection due to a large dielectric constant contrast between steel and concrete.
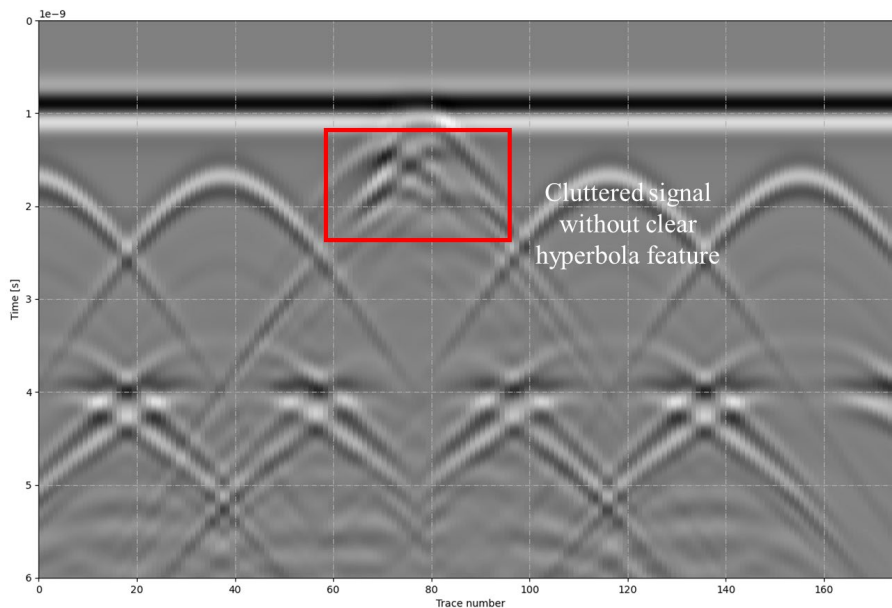

Figure 3-3. GPR Signatures of Reinforcement Concrete Deterioration with Cracks Filled with Water

Figure 3-4 shows synthetic GPR B-scans for shallow delaminations with different widths. The width of simulated delaminations varies from 0.1mm to 2mm. The delamination width smaller than 0.3mm is viewed as thin delamination in this report. The simulated results indicate that

the signature of thin delamination is not obvious in the GPR scan. For the thick delamination, a narrow band signature on the hyperbola peak is shown in the GPR scan. The results indicate that GPR has the potential to detect thick shallow delaminations in bridge deck. However, for thin shallow delamination, GPR has very limited capability to detect it.
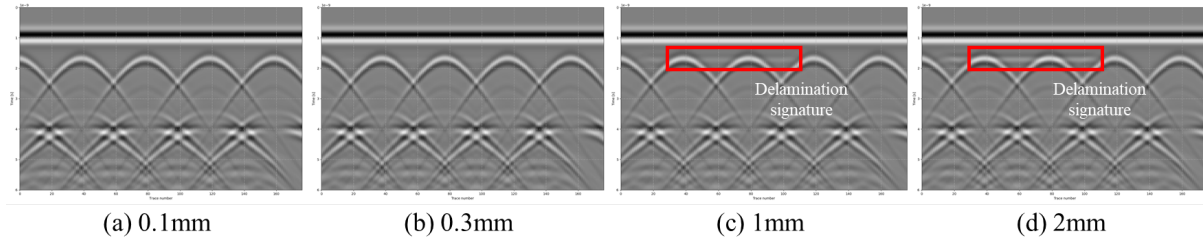

| (a) 0.1mm | (b) 0.3mm | (c) 1mm | (d) 2mm |

Figure 3-4. Synthetic GPR B-scans for Shallow Delamination

Figure 3-5 presents synthetic GPR B-scans for intermittent delamination. The simulated results indicate that the thin delamination signature is not visible on the GPR scan. The 1mm and 2mm delaminations show signatures on GPR scans. The intermediate delamination signature appears between two rebars, i.e., at the tails of two hyperbolas. Compared to shallow delamination, intermediate delamination is more difficult to detect in GPR scans. This is because that intermediate delamination is located below the first layer of reinforcement, the signature will only be visible between the space of rebars. In addition, the delamination signature intersects with hyperbola tails, which makes it more complex.
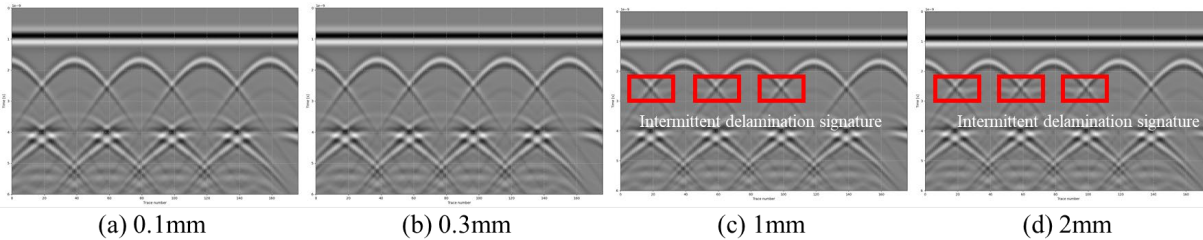

| (a) 0.1mm | (b) 0.3mm | (c) 1mm | (d) 2mm |

Figure 3-5. Synthetic GPR B-scans for Intermittent Delamination

Figure 3-6 presents synthetic GPR scans for deep delamination defects. The width of simulated delamination varies from 0.1mm to 2mm. The simulated results do not show evident signatures of deep delaminations in GPR scans. This can be explained in two aspects. First, GPR B-scan is very complicated to analyze for the area close to the bottom of the slab because reflections are coming from the two layers of reinforcement and the bottom of the slab. Second, the reflection from deep delamination is inherently weak due to signal attenuation caused by geometric and conductive losses. As a result, deep delamination is hard to detect solely based on the GPR B-scan.
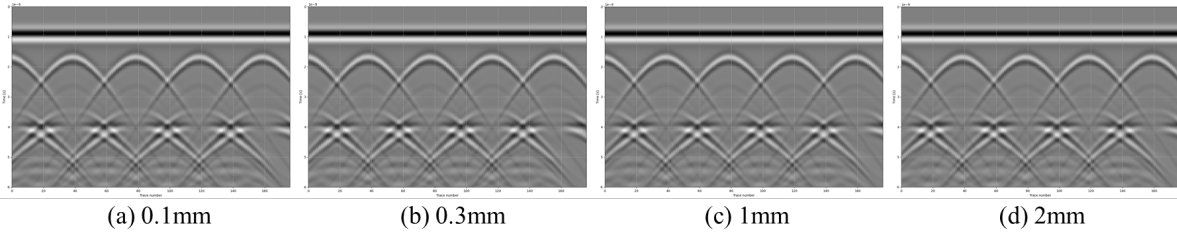
(a) 0.1mm   (b) 0.3mm   (c) 1mm   (d) 2mm

Figure 3-6. Synthetic GPR B-scans for Deep Delamination

The simulated results demonstrate the potential of GPR in reinforced concrete deterioration and thick delamination detection in the concrete slab. Among them, reinforced concrete deterioration shows weaker hyperbola reflection or indistinct hyperbola feature in a GPR scan. The delamination defects show signatures in a GPR scan at different locations depends on the type of delaminations. Since delamination is relatively more challenging to detect, a GPR survey was conducted on a concrete slab built with delaminations (Fig. 3-7). The concrete slab dimension is 1m × 1.1m, and the thickness is 200mm. The slab has two layers of steel reinforcement, and each layer consists of rebars in longitudinal and traverse directions. The top reinforcement is 65mm from the surface and the bottom reinforcement layer is 30mm from the slab bottom. Each reinforcement layer is composed of 13mm diameter rebars spaced at 200mm in both longitudinal and traverse directions.
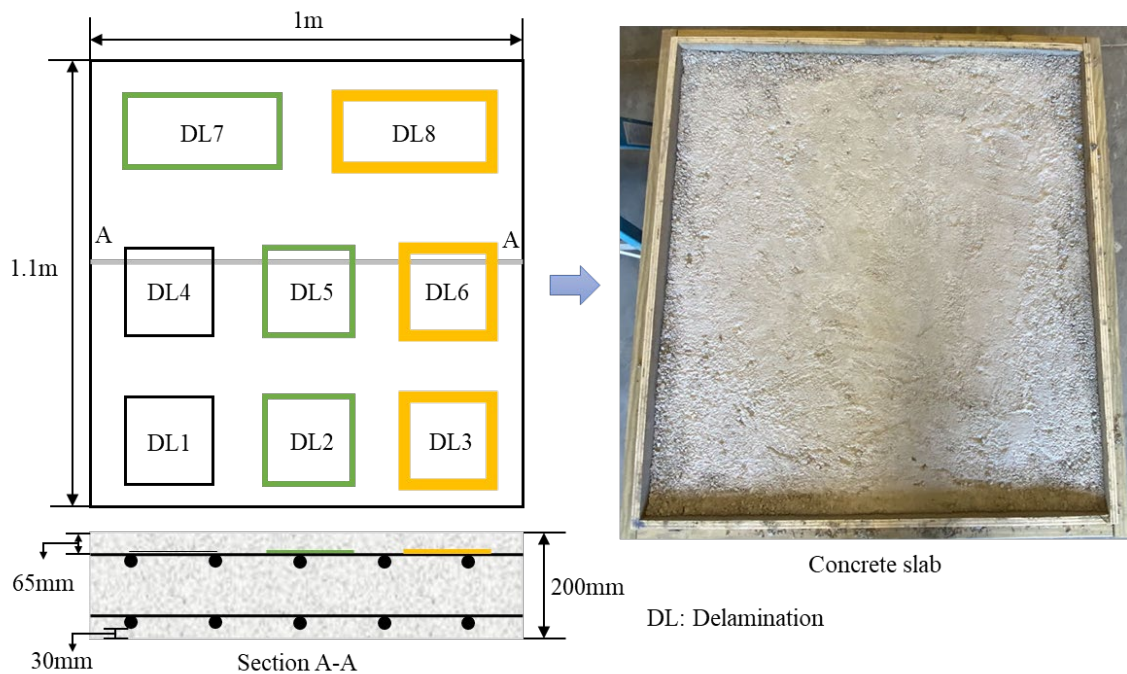
Figure 3-7. Schematic Diagram of Prefabricated Delaminations in Concrete Slab

A total number of 8 delaminations are embedded in the concrete slab. The prefabricated delaminations include three shallow, three deep, and two intermediate delaminations. Table VIII presents the characteristic of each delamination embedded at different depths. Figure 3-8 shows the process of delamination installation in the concrete slab. The depths of shallow, intermediate, and deep delaminations are 65mm, 130mm, and 170mm, respectively. The

delamination is represented using the polystyrene foam sheet. The polystyrene sheets were installed at designated positions during concrete slab pouring. The width of delamination varies from 2mm to 6mm. The 2GHz antenna was used to collect GPR data.

TABLE VIII
List of fabricated delaminations

ID	Size (mm)	Depth (mm)	Thickness (mm)
DL1	200×200	170	2
DL2	200×200	170	4
DL3	200×200	170	6
DL4	200×200	65	2
DL5	200×200	65	4
DL6	200×200	65	6
DL7	300×140	130	4
DL8	300×140	130	6

(a) Shallow delamination   (b) Intermittent delamination   (c) Deep delamination

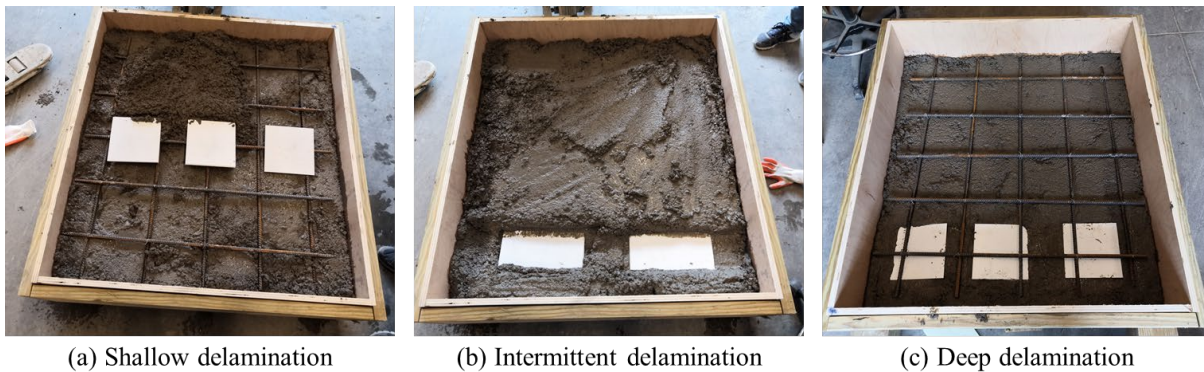**Figure 3-8. Fabricated Delaminations in Concrete Slab**

Figure 3-9 presents the detection results of delaminations in the concrete slab. The direction of GPR scan is approximately perpendicular to the direction of the top rebar mat. As illustrated, the band signatures of shallow delaminations with different widths are clearly visible in GPR scans. Since the shallow delamination always appears right on the top rebar mat, the band signature is connected to the hyperbola peak. The results indicate that the wider delamination has more significant features in GPR B-scan, which is consistent with the previous simulation. The intermediate delaminations DL7 and DL8 show very weak signatures in the GPR scans. However, the weak signature is hard to be concluded as delamination in practice since it is hard to differentiate from unwanted or noisy signals. For the deep delamination, DL2 and DL3 show some signatures but are barely recognized due to a reduced signal-to-noise ratio.
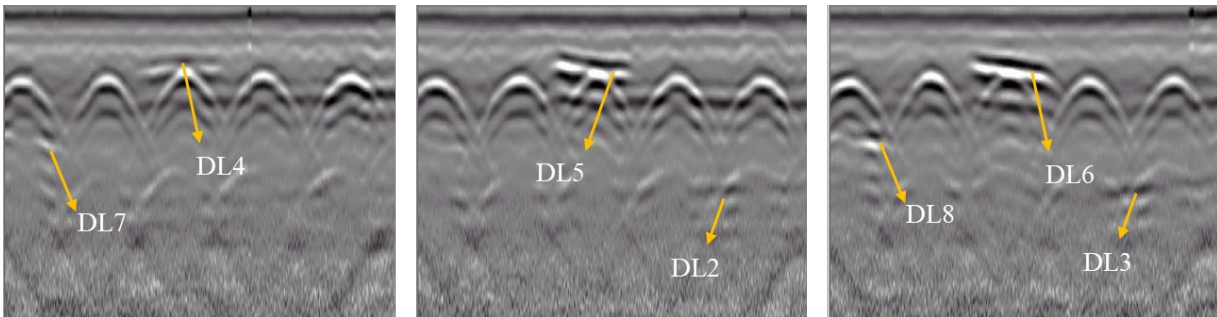
Figure 3-9. Detection of Delaminations (GPR Scan Perpendicular to the Direction of Top Rebar Mat)

Figure 3-10 presents the detection results from GPR scan along the direction of the top rebar mat. The results indicate shallow delamination can be clearly detected in the GPR scan. The intermediate delamination DL8 shows significant signatures in the GPR scan. However, delamination DL7 is not visible on the radargram. Deep delaminations DL2 and DL3 show weak signatures in the GPR scan at the space of two rebars. Delamination DL3 has a more significant signature than delamination DL2 due to a greater thickness. The GPR scans from two directions indicate that direction of GPR scan will affect the detection of intermediate and deep delaminations. The signature of shallow delamination is clearly visible from both directions. On the other hand, intermediate and deep delaminations are relatively hard to detect due to insignificant signatures in GPR scans.
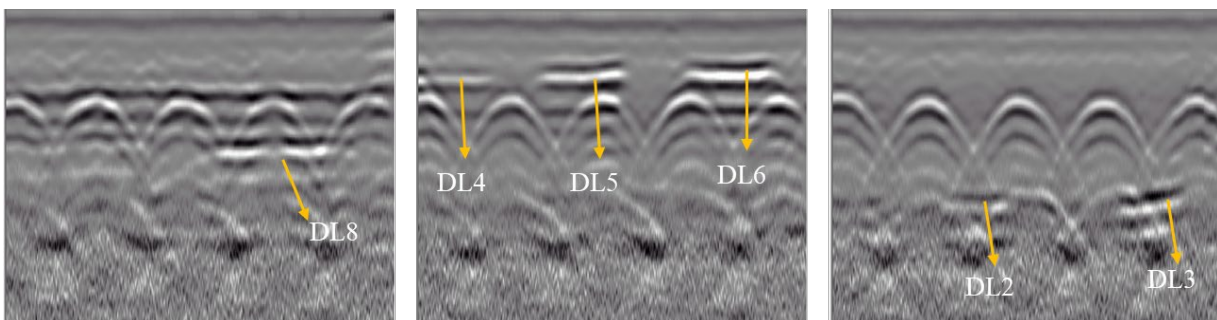

Figure 3-10. Detection of Delaminations (GPR Scan Along the Direction of Top Rebar Mat)

The GPR data analysis suggested that a GPR system has the potential to recognize reinforced concrete deterioration areas. These deteriorated areas show a weaker rebar reflection or indistinct hyperbola feature in the GPR B-scan, which can be used as indicators to assess bridge deck conditions. For thick shallow delaminations, a high-frequency GPR is shown to be a promising tool to recognize them based on their significant signature in the GPR scan. However, there remain challenges to be addressed for shallow delamination detection. First, the delamination is typically very thin and has an irregular shape in the real bridge deck. In this case, the signature of delamination will not be obvious and detectable. Moreover, field data always show noisy signals in the GPR scans, which further hinders the recognition of delamination signatures. For intermediate and deep delamination, even though some signatures are shown in the GPR scan, but these signatures are not very obvious and suffer from noisy signals at a greater depth. Therefore, using GPR to detect delamination, especially

intermediate and deep delaminations, in bridge decks remain challenging. Previous studies have indicated that shallow delamination will lead to more signal attenuation [20]. The signal attenuation will also lead to a weaker rebar reflection, which is similar to the corrosion of reinforcement and/or concrete deterioration. Therefore, a weak rebar reflection may come from either of these defects or a combination of them. In this report, rebar reflection amplitude will be used as an indicator to assess bridge deck conditions. The next chapter will elaborate on the method to automate rebar detection and deterioration map generation.

Chapter 4 Methods and Results

A workflow and associated tools were developed and tested to process GPR data and generate color-coded maps to indicate potential deterioration areas of bridge decks. The developed tools could automate the processing of a large amount of GPR data, thus reducing time and labor costs and facilitating the adoption of GPR in bridge deck inspection and deterioration assessment. Figure 4-1 provides an overview of the proposed method that consists of three steps. First, the random forest classification model [39] was trained to detect rebar regions in GPR scans using the features obtained from histogram of oriented gradients (HOG) [40]. The rebar region is the region in a GPR scan that contains a hyperbolic signature representing the reflection from a rebar. The peak of hyperbola represents the rebar position. Second, a robust hyperbola fitting method was used to fit hyperbola signature in each rebar region. The position of rebar can then be estimated by finding the peak of the fitted hyperbola. The amplitude at the rebar location can then be extracted for subsequent condition assessment. Third, the signal amplitudes at rebar locations were normalized. Considering the surface conditions, the average direct-coupling amplitudes on the top of each rebar region was computed and used. Fourth, depth correction was conducted to reduce the effects of rebar depth on signal attenuation of rebar reflection, such that the adjusted rebar amplitudes can be used as an indicator for bridge deck condition assessment. Finally, deterioration map was generated using depth-corrected amplitudes, in which weak reflection and small signal amplitudes may indicate potential deterioration areas of a concrete bridge deck.
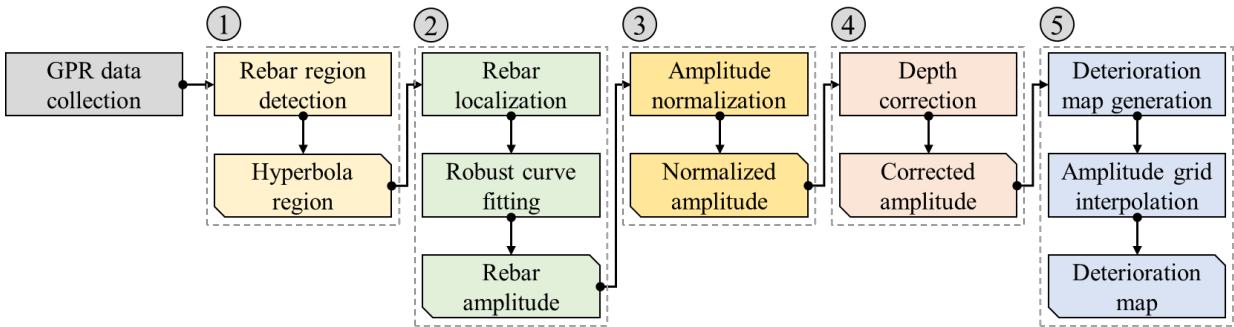

Figure 4-1. Method Overview

The developed workflow and tools for processing GPR data were validated in three case studies. Three bridges were surveyed using a GSSI SIR-4000 GPR system with a 2GHz ground-coupled antenna unit and parameters suggested in Chapter 3. The purpose is two-fold. First, using the actual GPR data collected from the bridge decks, the developed tools for rebar detection can be tested and evaluated. A total of 2010 rebar features from the GPR data were selected to evaluate the accuracy of the proposed detection method. The method achieved an accuracy of 98.6%, demonstrating its effectiveness. Second, the workflow of using GPR to survey bridge deck, processing collected GPR data, generating color-coded deterioration maps were validated through the case studies. The generated deterioration maps can then be used by professionals to further inspect and evaluate bridge decks. For example, detailed examinations and tests can be conducted at the "hot spots" on the deterioration maps.

The following sections provide details on the proposed method and case studies.

4.1 Automated Rebar Region Detection

The Random Forest (RF) approach [41] was adopted to detect hyperbolic features in GPR scans that represent rebars in a bridge deck. The RF approach is a supervised classification algorithm that uses bootstrap aggregating (bagging) with random feature selection (Figure 4-2). The RF method fits a number of decision tree classifiers on sub-training datasets of the entire dataset, and averages these trees to improve model performance and avoid over-fitting issues. The bootstrap method, a resampling technique [42], is used to de-correlate the trees with different resampled training sets. The bootstrap method can decrease the variance of the model without introducing bias and improve the performance of the classification model.
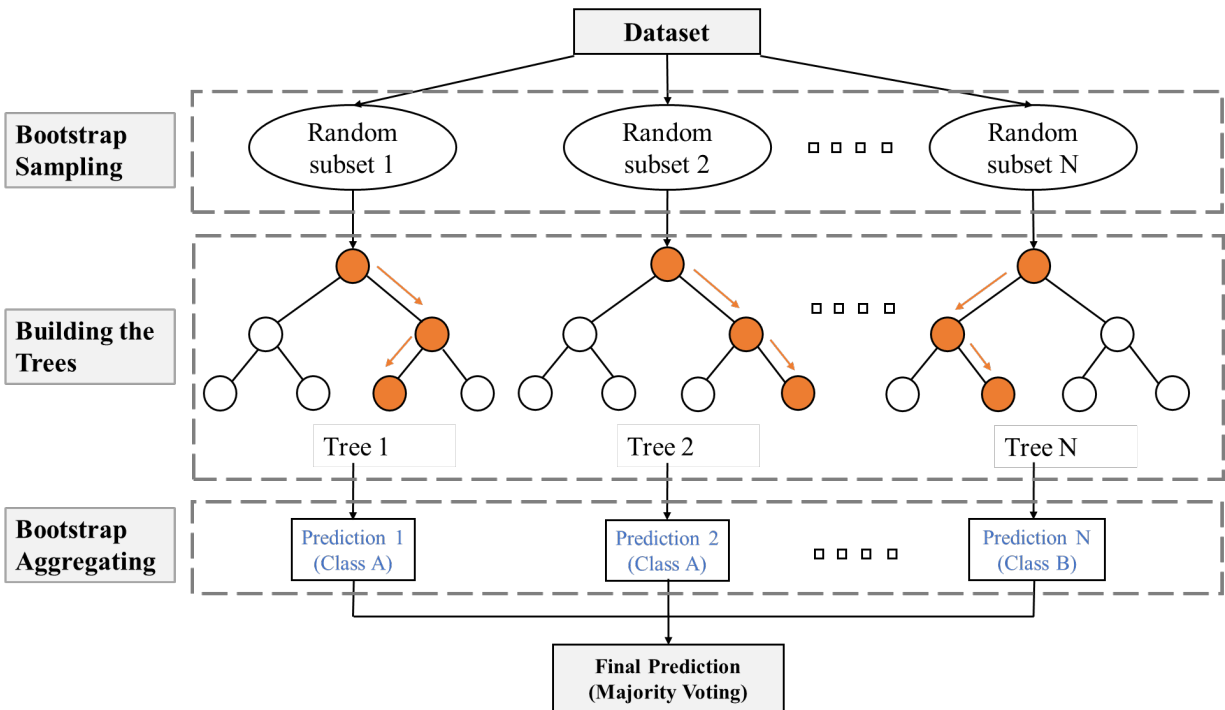
Figure 4-2. Schematic of Random Forest Approach

The histogram of oriented gradients (HOG) was used to compute features of the training dataset. The HOG is a dense feature extraction method [40] that has been widely used in computer vision. The calculation of HOG feature descriptor consists of three steps. In the first step, the gradient for every pixel in the image is computed in both horizontal and vertical directions. This is achieved by filtering the image with filter kernel $[-1,0,1]$ and $[-1,0,1]^T$. The magnitude g and direction θ of gradient can be calculated using Eq. (6), where g_x and g_y are the horizontal and vertical gradients, respectively.

$$\begin{cases} g = \sqrt{g_x^2 + g_y^2} \\ \theta = \arctan\dfrac{g_y}{g_x} \end{cases} \tag{6}$$

In the second step, histogram of gradients is calculated to obtain feature matrix for each cell. Every pixel casts a weighted vote on an orientation-based histogram. The third step normalizes

feature matrix across blocks using L2 norm method shown in Eq. (7). v is the feature vector, $\|v\|_2$ represents 2-norm for vector v.

$$f = \frac{v}{\sqrt{\|v\|_2^2 + \varepsilon^2}} \qquad (7)$$

To train an RF classifier, both positive and negative classes were prepared. Specifically, the positive class is the sample with rebar regions, and the negative class is the sample without rebar regions. The training image dataset has a fixed 32×52 pixel size. Figure 4-3 presents examples of the training dataset. A total number of 1500 positive samples and 3000 negative samples were collected and prepared.
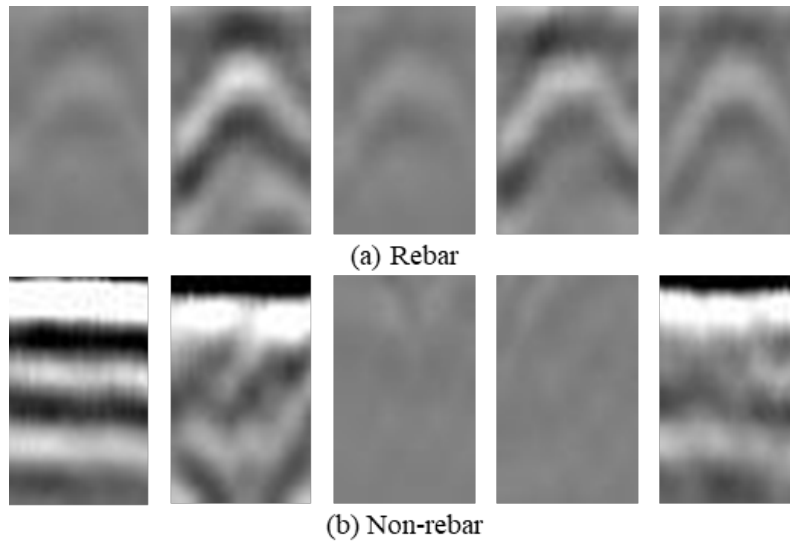

(a) Rebar

(b) Non-rebar

Figure 4-3. Examples of Training Samples (32×52)

In this report, the sample is divided into 4×4 pixel cells. The magnitudes of these 16 pixels in each cell are binned and cumulatively added into 9 buckets of unsigned direction. In addition, a 2×2 cell block is used to slide across the image. A 32×52-pixel image has 84 blocks of 8×8 pixels. Each of these 84 blocks has a 36×1 feature vector. Therefore, the total number of features for the image is 84×36=3024. The HOG features are scale-invariant when the aspect ratio of the hyperbola signature is constant. Typically, the cover thickness of the top rebar is around 5cm to 7cm. The spacing of reinforcement is between 15cm to 30cm [6]. Furthermore, the diameter of rebar in a bridge deck varies between 12mm to 15mm [43]. Thus, the hyperbola signatures for different bridges are similar to each other.

The trained model can be used to detect regions with hyperbola features, i.e., the rebar region in GPR scans. A moving 32*52 sliding window moves from top left to bottom right to extract the sample. The sample will be classified as the rebar or the non-rebar region. Figure 4-4 presents the detection of the hyperbola features in GPR scans. Multiple bounding boxes are generated around each hyperbola. To refine the results, the Non-Maximum Suppression (NMS) technique [44] was used to reduce redundant detections and avoid false positives.
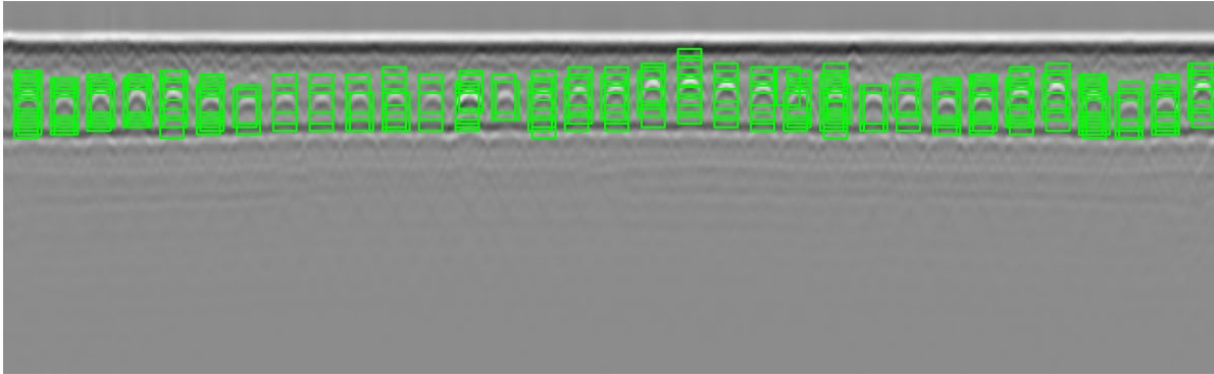
Figure 4-4. Exemplary Results of Raw Hyperbola Feature Detection

The input for the NMS method is a list of proposal boxes B, corresponding confidence scores and overlap threshold N. The output is a list of filtered proposals D. The method consists of five steps:

1. Choose the proposal with the highest probability from list B and add it to filtered proposal D. (D is empty at the beginning.)
2. Compare selected proposal in filtered proposal D with each of proposal in list B by calculating the Intersection over Union (IOU) score. If the IOU is greater than the threshold value, remove that proposal from B to list D.
3. Select the proposal with the highest probability from list B and remove it from B to D.
4. Compute the IOU score of this proposal with others in list B and eliminate proposal with an IOU value higher than threshold N.
5. Repeat steps 1 - 4 until no proposals in list B.

Figure 4-5 shows the final detection results after NMS. This processing step can remove redundant bounding boxes. Each bounding box represents a potential rebar region.
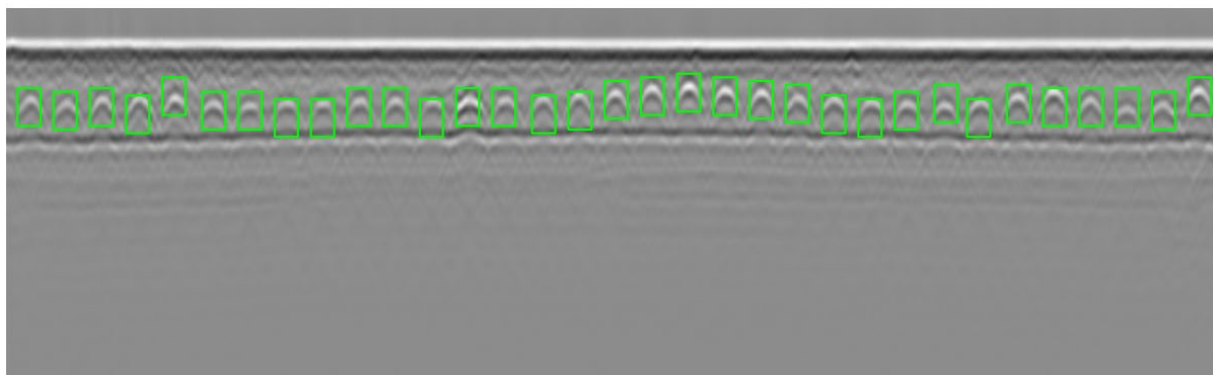
Figure 4-5. Final Detection Results After NMS

4.2 Rebar Localization

The rebars are reflected as hyperbola features in a GPR scan and the hyperbola peak represents the rebar location [45]. Hence, a hyperbolic curve fitting method [46] was used to fit the hyperbolic feature and identify the peak of hyperbola. The maximum intensity point in each continuous A-scan forms the hyperbola in a B-scan. Therefore, the coordinates of the points with the maximum intensity in each column within each rebar region were extracted to

fit the hyperbola. The hyperbola is defined in Eq. (8), where (h, k) is the center of hyperbola, a is semi-major axis length, b is semi-minor axis length. The hyperbola peak coordinate is (h, k+b).

$$\frac{(y-k)^2}{b^2} - \frac{(x-h)^2}{a^2} = 1 \tag{8}$$

However, outlier points in each rebar region may affect the hyperbola fitting result, resulting in inaccurate rebar localization. To overcome this issue, the nonlinear hyperbola fitting was formulated as an optimization problem by introducing a sublinear function $\rho(z)$. Eq. (9) shows the optimization formulation, where (x_i, y_i) represents point coordinates, **P** is the fitting parameter vector, and $\varphi(\mathbf{x}; \mathbf{P})$ is the hyperbola function defined in Eq. (8).

$$\frac{1}{2}\sum_1^n \rho\left(\left(\varphi(x_i; \mathbf{P}) - y_i\right)^2\right) \to \min_{\mathbf{P}} \tag{9}$$

The smooth approximation method named 'soft L1 loss' [47] is used to implement the function ρ, which has been demonstrated to be effective for robust least squares. The 'soft L1 loss' is defined in Eq. (10).

$$\rho(z) = 2\left(\sqrt{1+z} - 1\right) \tag{10}$$

Figure 4-6 shows the results of hyperbola fitting with the presence of outliers due to signal noises. The results indicate that the robust hyperbola fitting method can accurately fit the hyperbola and find the hyperbola peak. However, normal hyperbola fitting using Eq. (8) leads to skewed fitting results and incorrect rebar location.

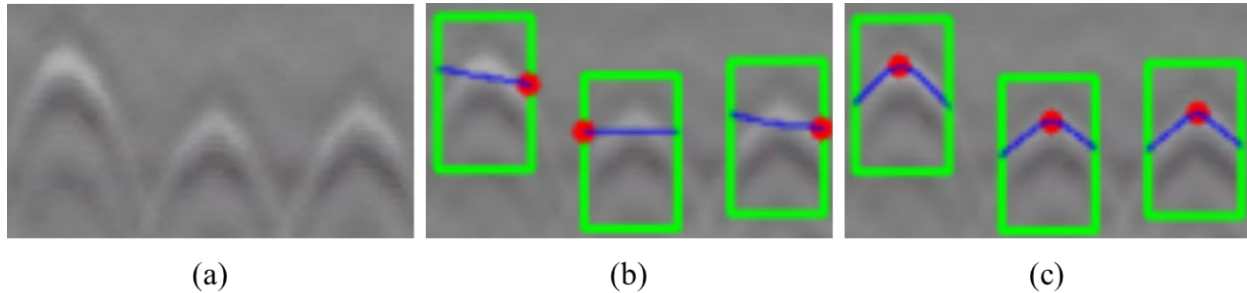(a)   (b)   (c)

Figure 4-6. Hyperbola Fitting with Outliers. (a) Original Image; (b) Hyperbola Fitting; (c) Robust Hyperbola Fitting (Blue Curve Represents Fitted Hyperbola Curve; Red Circle Is the Hyperbola Peak)

Figure 4-7 presents the results of robust hyperbola fitting for GPR scans of a bridge deck. The hyperbola peak is correctly estimated, which represents the potential rebar location. The corresponding amplitude, location, and two-way travel time (TWTT) of each rebar were extracted for further normalization and depth correction analysis.
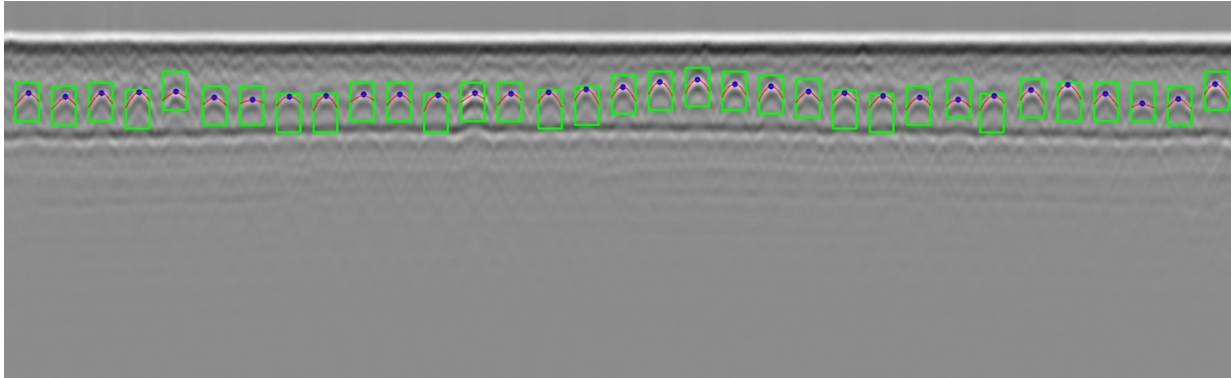
Figure 4-7. Exemplary Results of Rebar Localization

The rebars are placed in a concrete bridge deck with uniform space to reinforce and strengthen cast concrete. Therefore, obvious hyperbola features are expected in GPR scans for specified spacing *S*. Bridge deck deterioration may lead to blurry signatures or even the absence of hyperbolical features, which are difficult to be detected using the proposed method. These potential deterioration areas cannot be ignored. Therefore, a method to avoid missing rebar detection was developed. First, the rebar spacing *S* was estimated using the clear rebar features in a GPR scan. The spacing can be calculated as the average distance between adjacent hyperbolas in a GPR scan. Second, the distance between adjacent rebars detected by the method was calculated. If the distance *d* between adjacent rebars is greater than 1.8 times spacing *S*, rebar signatures need to be placed in the GPR scan between the two adjacent rebar signatures detected by the method. If there is one missing rebar signature between two adjacent rebars detected in a GPR scan, the distance between the detected rebar signatures should be 2 times spacing S. For estimation purpose, the value of 1.8 was selected in order to determine whether a region is missing a rebar signature. The number of missing rebar signatures *N* can be calculated in Eq. (11).

$$N = round\left(\frac{d}{S}\right) \tag{11}$$

Finally, missing rebar signatures were added by first estimating the rebar regions in the GPR scan. The region position was interpolated by the detected hyperbolas of adjacent rebars. Since there is no clear hyperbolical feature in the region, the hyperbola fitting method is not applicable to locate the rebar. The position with the maximum reflection amplitude around the middle in that region was assumed to be the rebar location. The assumption is made based on two reasons. First, steel rebar yields strong reflection in the concrete due to a large relative permittivity value. Though corroded rebar or deteriorated concrete leads to a weaker reflection, the permittivity difference can still result in a relatively larger reflection compared to non-rebar region. Second, reinforcing rebars are designed to place in the concrete bridge deck with uniform spacing. Correspondingly, the rebar position detected from GPR scans should also have approximately equal spacing. Hence, the rebar should be in the middle of the interpolated region. Figure 4-8 shows an example of the output of the proposed method.
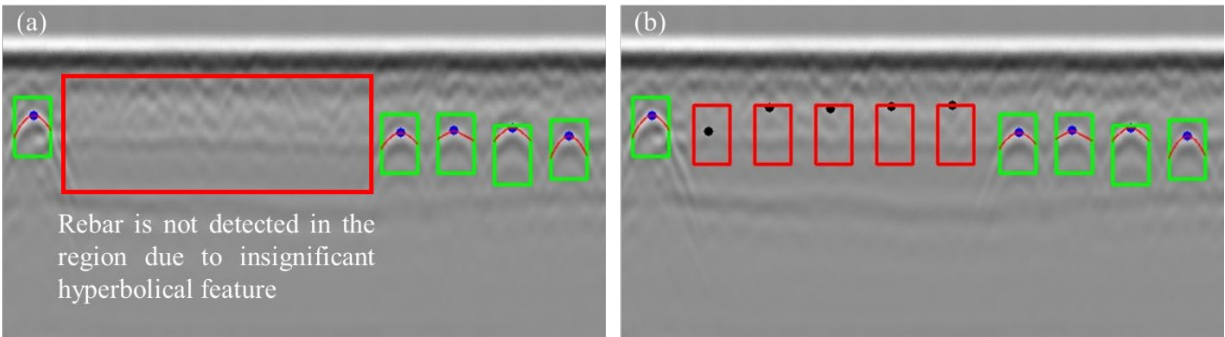
Figure 4-8. Exemplary Results of the Improved Method Considering Missing Detections

The method may detect some regions with hyperbolical features, but they are not belonging to top rebar mat. These false positives may affect the determination of deteriorated areas in concrete bridge decks. Therefore, false positives need to be removed from the final detection to ensure an accurate condition assessment. The removal of redundant detection is based on the following criteria.

1. If the two-way travel time of the detected rebar is larger than 3.5ns, the rebar is treated as a false positive and will be removed. This is because that the permittivity of concrete varies from 4 to 11, 3.5ns two-way travel time translates into a distance from 15.7cm to 25.4cm, which is much greater than the typical cover thickness of rebar in bridge design. Therefore, 3.5ns can ensure the method will not delete true positives.

2. If there are two detected rebar regions with spacing smaller than 20 traces, the rebar with a smaller travel time will be kept. This is because rebar reflections only come from the top rebar mat are used to assess bridge deck condition. In addition, the selection of 20 traces is reasonable, based on that, the rebar spacing is greater than this value. Therefore, one of the two detected rebars is redundant that needs to be deleted.

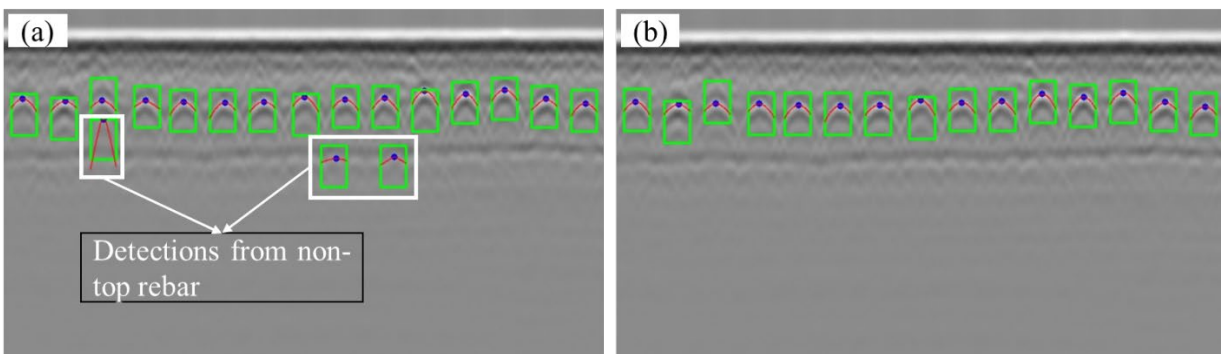Figure 4-9 presents examples of rebar detection without redundant detection.

Figure 4-9. Examples without Redundant Detection

4.3 Rebar Reflection Amplitude Normalization

Measured signals are typically normalized by a reference amplitude, and thus converting signal amplitudes to the same range. Traditionally, the reference amplitude is the maximum possible

value, which is 32,767 for 16-bit data and 4,294,967,296 for 32-bit unsigned long int data. The GPR data is converted to decibel scale through normalization. However, this method does not consider surface conditions. Surface defects such as patch and crack can affect direct-coupling reflection and rebar reflection amplitude. Figure 4-10 shows the raw GPR A-scan at the hyperbola peak of rebar. The direct-coupling reflection amplitude has the highest reflection amplitude as shown in the figure.
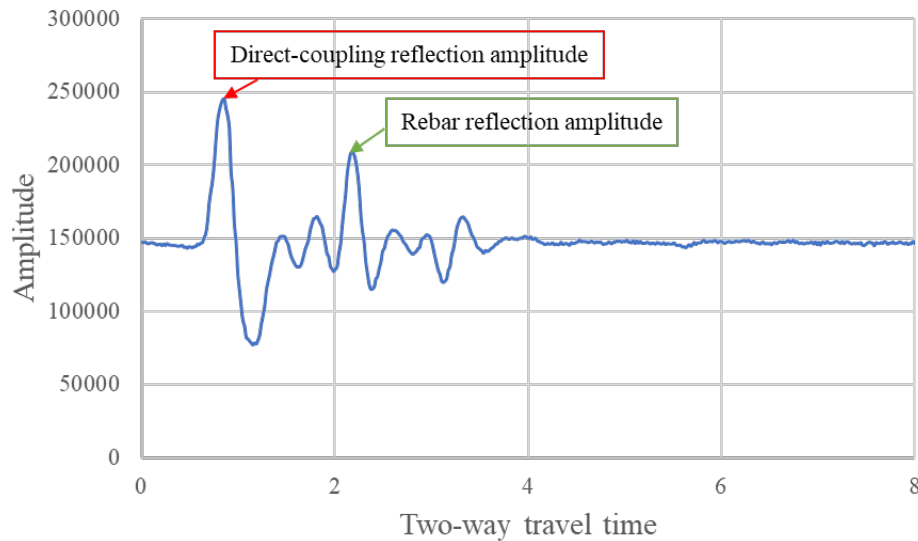
Figure 4-10. Raw GPR A-scan Over a Rebar

In this report, average direct-coupling amplitude on top of each rebar region was used to normalize rebar reflection. Figure 4-11 shows the spacing used to calculate the average direct-coupling amplitude for each rebar region. It is located on the top of the detected bounding box of rebar region. The length is 32 traces.
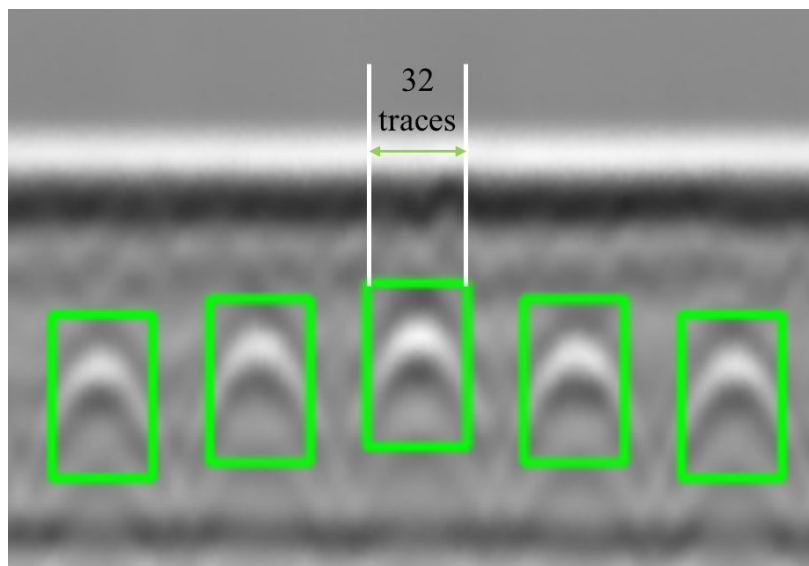

Figure 4-11. Direct-Coupling Amplitudes Used for Normalization

Eq. (12) illustrates the method to normalize rebar reflection amplitudes, where A_r represents the rebar reflection amplitude, A_s is the reference amplitude. The equation is used to normalize amplitude to decibel scale.

$$A_{norm}=20\times\log_{10}\left(\frac{A_r}{A_s}\right) \tag{12}$$

Figure 4-12 compares the proposed normalization method to the traditional approach using maximum possible reference amplitude. Figure 4-12(a) shows the rebar reflection amplitudes normalized against the maximum possible amplitude 4,294,967,296 for 32-bit unsigned long int data. Figure 4-12(b) plots the rebar amplitudes normalized by the average direct-coupling reflection amplitude above each rebar. The proposed method results in higher normalized amplitudes because each rebar reflection amplitude is normalized by its corresponding reference amplitude which is smaller than maximum possible amplitude. By incorporating individual rebar-specific reference amplitude, it is possible to mitigate the effect of surface anomalies on deterioration analysis.
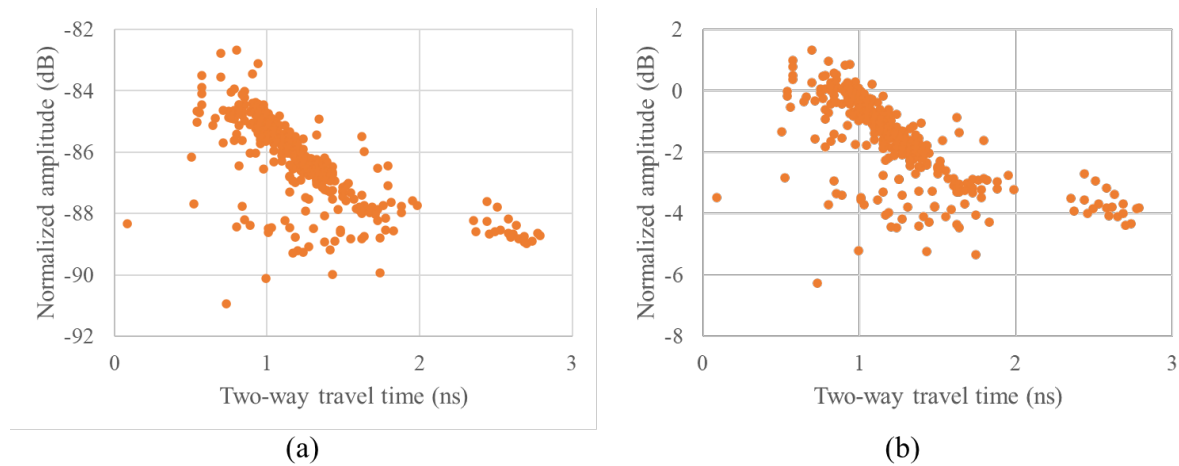

(a)   (b)

Figure 4-12. Scatter Plots of Rebar Amplitude vs. TWTT Normalized. (a) Traditional Approach (b) the Proposed Method

4.4 Depth Correction

The cover thickness of rebar in a bridge deck varies at different locations because rebars often deviate from their designated positions. These variations will affect rebar reflection amplitudes because a greater cover thickness will lead to greater energy loss, and thus leading to a weaker rebar reflection amplitude. Because that deterioration and increased rebar depth both contribute to the attenuation of reflected amplitude, therefore depth correction is a critical step to obtain a correct deterioration map. The depth variation effect needs to be eliminated to achieve an accurate assessment of bridge deck condition. In this study, the relationship between rebar reflection amplitude and its depth was developed. In [17], it was found that the rebar reflection amplitude in decibel scale is linearly correlated with rebar depth. However, accurate rebar depth is always not attainable solely based on GPR data. To address this issue, the relationship between TWTTs and reflection amplitudes in decibel scale of rebars was used

in this study [17]. The rebar depth effect on the bridge deck deterioration analysis can be mitigated using this relationship.

In this study, RANSAC linear regression [48] is used to model the relationship between TWTTs and rebar reflection amplitudes. RANSAC is more appropriate than linear regression in this case since many outliers are present in the data. The residual threshold for a data sample to be classified as an inlier or outlier is set as 1. The maximum number of iterations for random sample selection is 2000. Figure 4-13 shows the comparison of linear fitting and RANSAC robust fitting. The results indicate that the RANSAC fitting method can exclude the outliers and fit the model using inlier samples. The depth effect is corrected by adjusting the slope angle of the fit line to zero. The RANSAC fitted line has a slope of -4.16dB/ns. The negative slope could be attributed to depth variation of rebars and signal attenuation due to corrosion of rebars and/or concrete deterioration. If the bridge deck is in good condition, the amplitude decreasing with TWTTs can be considered as the effect of depth variation of rebars. Therefore, the amplitude must be corrected to represent the condition of the bridge deck. If the amplitude is low after correction, it is an indicator of concrete deterioration and/or corrosion of rebars.
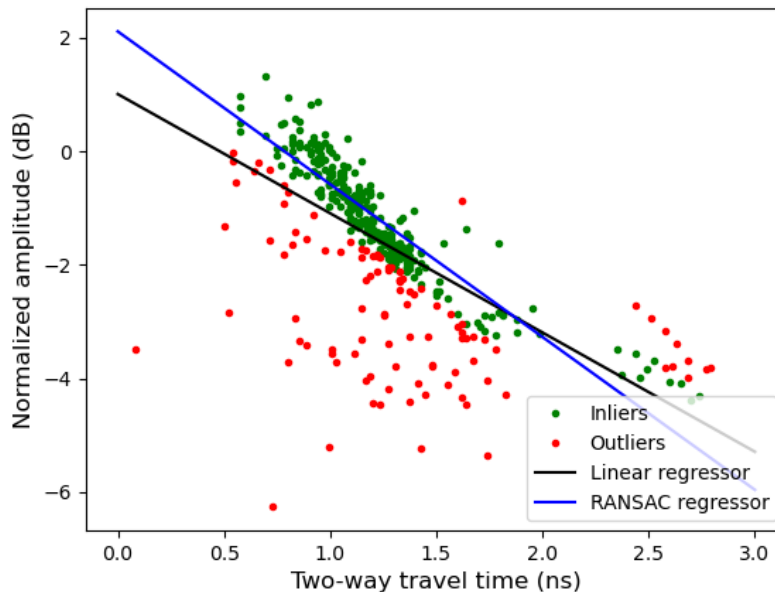

Figure 4-13. Scatter Plot of Amplitude Versus TTWT and RANSAC Line Fit (Each Point Corresponds to a Rebar)

The amplitude threshold value needs to be determined to identify potential deteriorated areas. If the bridge deck is in sound condition, rebar reflection amplitudes should follow a normal distribution [49]. The deterioration of the bridge deck will slightly shift the amplitude distribution to the negative side [49]. Median Absolute Deviation (MAD) around the median [50] is adopted to detect outliers in the distribution. Specifically, the amplitude that is 3-fold-scaled MAD below the median is considered as deteriorated areas [49]. Based on this condition, -0.84 dB is selected as the threshold value to determine whether the area has deteriorated or not. Figure 4-14 shows the threshold value for potential deterioration areas after depth correction.
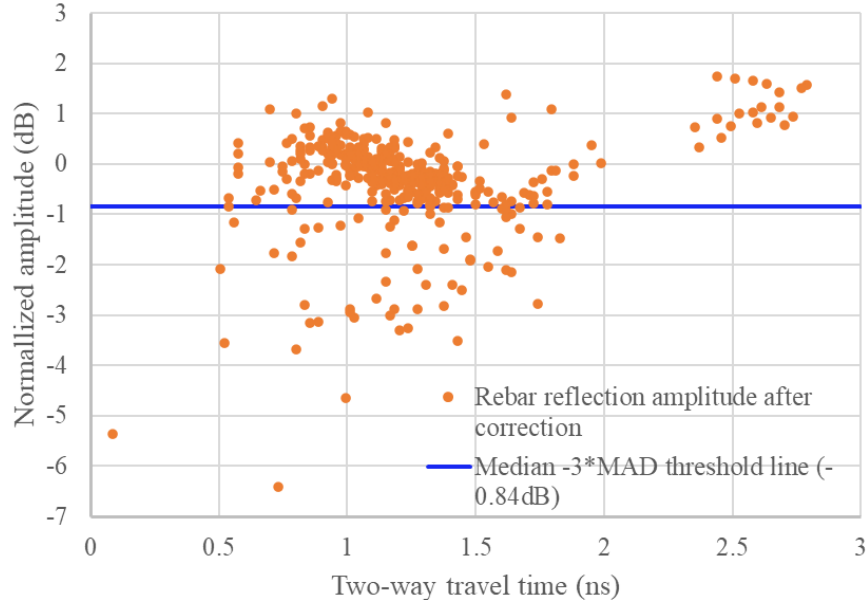
Figure 4-14.Threshold Value for Deterioration After Depth Correction

4.5 Deterioration Map Generation

The locations (X, Y) and depth-corrected reflection amplitudes of rebars are saved in ASCII file format. The coordinate system (X, Y) is in the bridge deck surface plane. The python programming language is used to create the color-coded deterioration map of the bridge deck. The color-coded deterioration map can help professions identify potential deterioration areas. The generation of deterioration map consists of two steps. In the first step, a rectangle grid out of an array of x values and an array of y values is created. The greater the number of grids, the higher the contour map resolution. Correspondingly, the interpolation time will be longer for a great number of grids. In the second step, amplitude values on the grid are interpolated by the collected rebar locations and amplitudes. Triangulation is first conducted on the input data with the Qhull method [51]. The interpolant is then constructed by performing linear barycentric interpolation on each triangle. Eq. (12) gives the calculation of grid node amplitude value inside a triangle, where Amp_i is the interpolated amplitude for node (x_i, y_i), A_1, A_2, and A_3 are reflection amplitudes for triangle vertex (X_1, Y_1), (X_2, Y_2), and (X_3, Y_3), W_1, W_2, and W_3 represent the weight. Finally, a contour map can be generated using the grid map with interpolated amplitudes [51].

$$\begin{cases} Amp_i = W_1 A_1 + W_2 A_2 + W_3 A_3 \\ W_1 = \dfrac{(Y_2 - Y_3)(x_i - X_3) + (X_3 - X_2)(y_i - Y_3)}{(Y_2 - Y_3)(X_1 - X_3) + (X_3 - X_2)(Y_1 - Y_3)} \\ W_2 = \dfrac{(Y_3 - Y_1)(x_i - X_3) + (X_1 - X_3)(y_i - Y_3)}{(Y_2 - Y_3)(X_1 - X_3) + (X_3 - X_2)(Y_1 - Y_3)} \\ W_3 = 1 - W_1 - W_2 \end{cases} \qquad (12)$$

4.6 Case Studies

The proposed workflow was validated for processing GPR data collected in three bridges. The GPR system configurations were set as follows. The antenna frequency is 2GHz, the horizontal parameter is 362 scans per meter, the samples per trace is 512, the time range is 7ns, the spacing of GPR scan is 0.46m, and the scanning direction is perpendicular to the top rebar mat. Figure 4-15 shows satellite images of the three bridges.

(a) Bridge ID #1

(b) Bridge ID #2
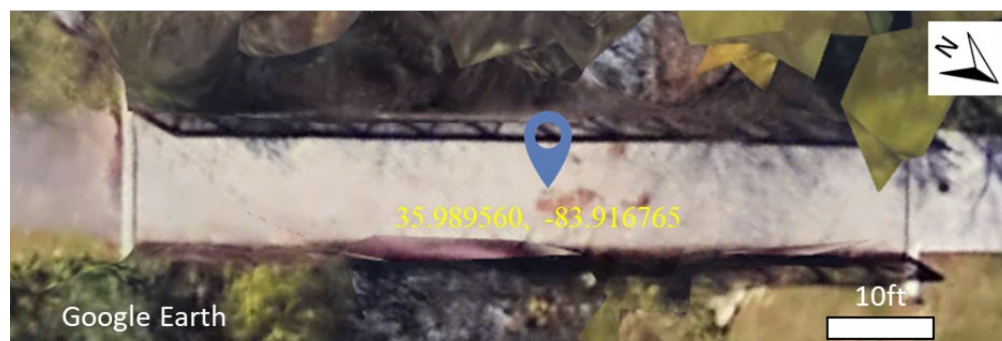
(c) Bridge ID #3

Figure 4-15. Google Map Image of the Three bridges (Map Data ©2021 Google)

Figure 4-16(a) presents the scatter plot of rebar reflection amplitude versus two-way travel time (TWTT) for the data collected from the three bridges. RANSAC linear regression was used to model the relationship between TWTTs and rebar reflection amplitudes. The residual threshold for a data sample to be classified as an inlier or outlier is set to 1. The maximum number of iterations for random sample selection is 2000. Figure 4-16(b) displays depth-corrected reflection amplitude versus TWTT for the three bridges.
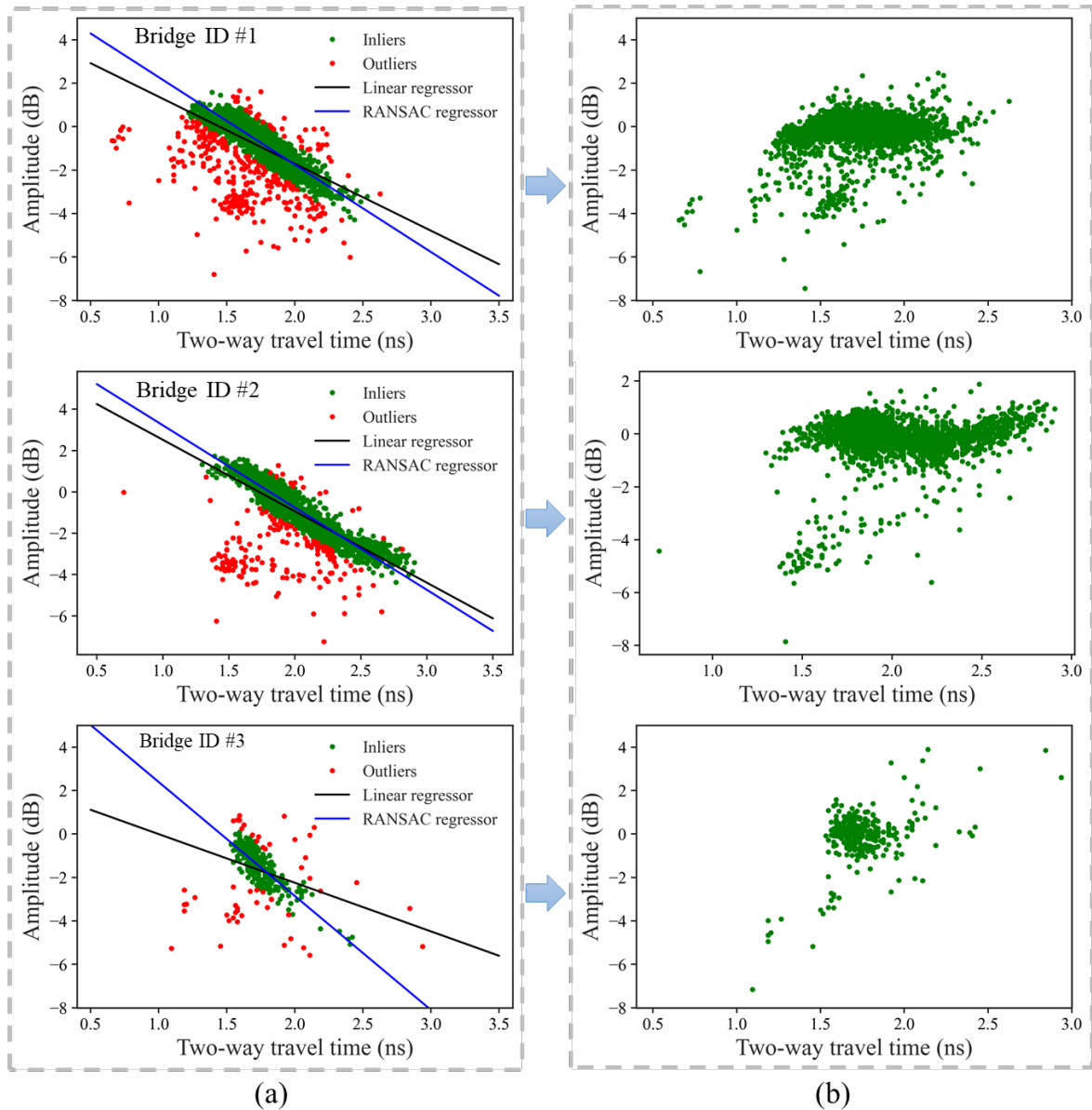
Figure 4-16. Depth Correction for the Three Bridges: Each Point Corresponds to a Rebar. (a) Scatter Plot of Amplitude Versus TTWT and RANSAC Line Fit; (b) Depth-Corrected Amplitude.

Histograms of the depth-corrected rebar reflection amplitudes from the three bridge decks are shown in Figure 4-17. The areas are considered to have deteriorated if amplitudes are 3-fold-scaled MAD below the median. As a result, -1.01 dB, -0.99 dB, and -1.10 dB are calculated as threshold values (i.e., determine whether the area has deteriorated or not) for Bridge ID #1, #2, and #3, respectively.

(a) Bridge ID #1   (b) Bridge ID #2   (c) Bridge ID #3

Figure 4-17. Histogram of the Rebar Reflection Amplitude of the Three Bridges

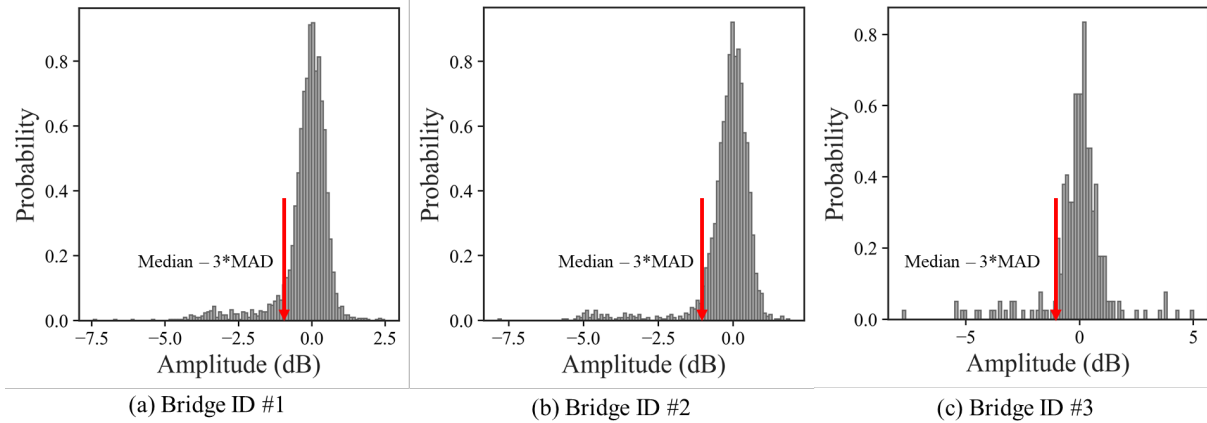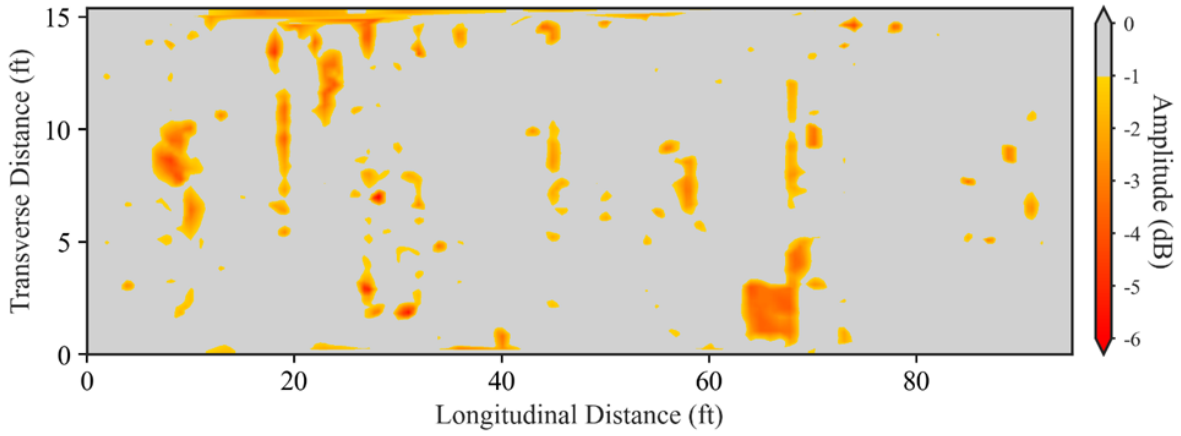Figure 4-18 shows deterioration maps of the three bridges. The deterioration map is generated to represent potential deteriorated areas, which is a contour map of rebar reflection amplitudes. The potential deterioration could be corrosion of reinforcement, concrete deterioration, or a combination of them. It should be noted that the deterioration map generated by the GPR data needs to be further validated by comparing to core samples taken from the bridge deck or other examination methods. In the deterioration map, the gray color indicates areas that have no obvious deterioration. Weaker rebar reflections are mapped as hotter colors which is an indicator of deterioration in these areas. The hotter color may indicate potentially more severe deterioration. Table IX presents the statistics of the deteriorated areas for the three bridge decks.

TABLE IX
Statistics of bridge deck deterioration

Bridge ID	Deteriorated areas (m²)	Percentage of total deck areas
1	12.4	9%
2	8.1	8%
3	6.4	8%

(a) Bridge ID #1
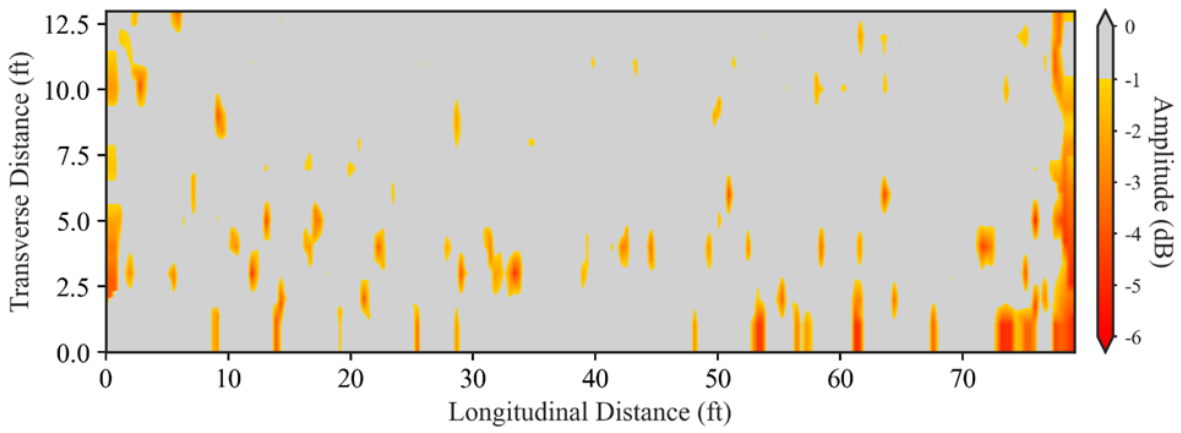
(b) Bridge ID #2

(c) Bridge ID #3

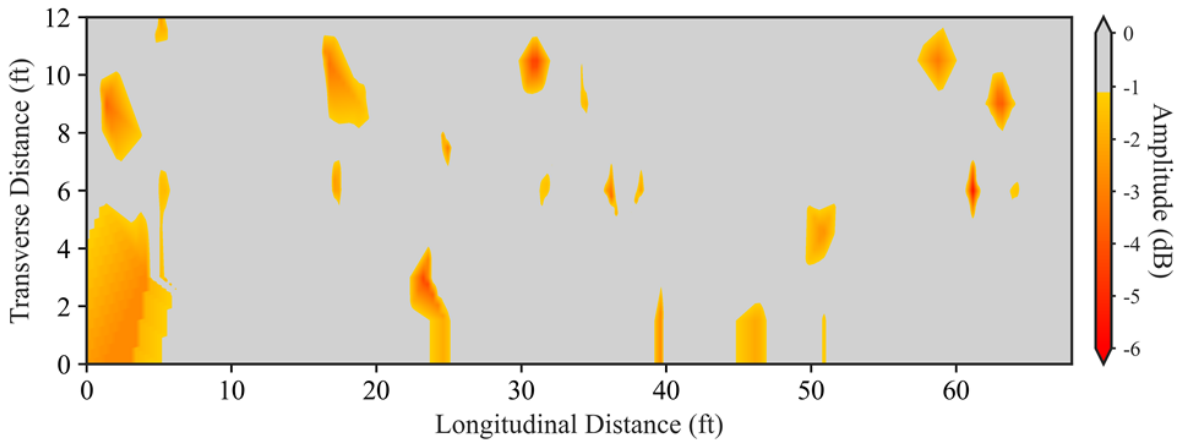**Figure 4-18. Deterioration Maps of the Three Bridges**

Chapter 5 Summary and Future Work

This study aims to investigate the potential of using GPR to inspect concrete bridge deck and assess potential deterioration, and develop tools to process GPR data and visualize bridge deck deterioration information to help improve bridge inspection and asset management processes. To this end, the research team first investigated GPR system configurations and scanning parameters that are suitable for concrete bridge deck inspection. Appropriate GPR system configuration and suitable scanning parameters were suggested to enable efficient collection of high-quality GPR data for bridge deck inspection. Second, GPR data of reinforcement concrete deterioration and delamination were collected, and the signal patterns were studied via computer simulations and laboratory experiments. Third, a workflow and associated tools were developed and validated in this study to help process collected GPR data for concrete bridge deck deterioration assessment. The random forest classification model was trained to detect rebar regions in GPR scans using features obtained from histogram of oriented gradients. Then, a robust hyperbola fitting technique was used to identify the hyperbola signature in each rebar region that indicates the rebar reflection and location. Finally, locations and depth-corrected amplitudes at the detected rebars were extracted as indicators for assessing potential deck deterioration. A color-coded map was used to represent the potential deteriorated areas of the bridge deck, which could help facilitate the inspection and evaluation of concrete bridge deck deterioration. To validate the workflow and the developed data processing tools, case studies were conducted to inspect three bridge decks and process the collected GPR data. The developed method achieved an accuracy of 98.6% in automatically identifying 2010 rebar features in the testing dataset.

The key findings and recommendations are summarized below.

- GPR system configurations and scanning parameters will impact GPR data collection efficiency and data quality. Based on the review of literature and practice, for concrete bridge deck inspection, GPR system with antenna frequency from 1.5 GHz to 2.6 GHz should be used. Scanning with the following parameters may produce good quality data in an efficient manner: 6-10 nanosecond (ns) time window, 512 samples per scan, 79 scans per meter, and 0.3-0.6m scan spacing. Scanning direction should be maintained perpendicular to the top rebar mat as much as possible.

- Using computer simulations and laboratory experiments, signal patterns of different bridge deck defects were investigated. It was found that rebar corrosion and concrete deterioration exhibit attenuated signal amplitudes or blurry hyperbolic features at rebar locations, which can be used to indicate potential deterioration areas. Delamination that has a thickness greater than 1mm developed at shallow depth in the bridge deck exhibits signatures in GPR scans. Delamination with a thickness smaller than 0.3mm in the bridge deck does not present noticeable signatures in the collected GPR scans, and thus is difficult to be detected.

- Detecting and locating rebars in GPR scans, and assessing the signal amplitude attenuation are critical steps to process GPR data to indicate the areas of potential deterioration in concrete bridge decks. A machine learning method based on random

forest classification and robust hyperbola fitting was developed to locate the rebar and extract the amplitudes for deterioration assessment.

- After signal amplitude normalization and depth correction, median absolute deviation can be used to set the threshold value to detect potential deterioration areas. Color-coded maps can visually represent and quantitatively estimate the bridge deck deterioration areas. The proposed methods and workflow were tested in case studies, confirming the potential of using GPR for concrete bridge deck inspection and assessment.

- GPR can be used as a complementing technique to existing methods for concrete bridge deck deterioration assessment. To expedite the use of GPR in bridge deck assessment, appropriate system configurations and scanning parameters should be used to ensure data collection efficiency, and automated processing methods should be used to reduce the efforts in manual analysis and interpretation. Estimating and visualizing potential deterioration areas of bridge deck from GPR scans should be implemented to provide quantitative information for inspection, asset management, and decision-making. GPR results should be carefully examined and interpreted when used for detecting and characterizing specific defects such as delamination. For complete and more accurate bridge deck deterioration assessment, GPR can be used in conjunction with other methods to improve the assessment performance.

Despite the demonstrated potential, future studies are needed to facilitate the use of GPR in concrete bridge deck inspection and assessment. First, bridge deck deterioration is a gradual process during the service period of bridges. Hence, periodic GPR data collection should be conducted, and effective methods should be developed to monitor potential bridge deteriorations from consecutive GPR scans of the same regions. Determining the thresholds of signal changes that indicate deck deterioration is the key. Continuous comparison of GPR signal changes and correlations with laboratory tests on core samples taken from bridge decks could help determine appropriate threshold for practical applications. Second, the proposed method relies on the detection of rebar and extraction of signal amplitude for assessing bridge deck deteriorations. It is effective in detecting defects such as rebar corrosion and severe concrete deterioration. However, defects such as delamination are difficult to be detected and characterized solely based on the proposed method and GPR data. Therefore, future studies could explore new sensing techniques and the fusion of multiple sensory data for more accurate and complete concrete bridge deck inspection and deterioration assessment.

References

[1]   D. Johnson, Tennessee Has 953 Structurally Deficient Bridges, (2018). https://patch.com/tennessee/nashville/tennessee-has-953-structurally-deficient-bridges-report (accessed April 21, 2021).

[2]   S. Kashif Ur Rehman, Z. Ibrahim, S.A. Memon, M. Jameel, Nondestructive test methods for concrete bridges: A review, Constr. Build. Mater. 107 (2016) 58–86. https://doi.org/10.1016/j.conbuildmat.2015.12.011.

[3]   D. Priya, Medium Frequency Ground Penetrating Radar (GPR), (n.d.). https://slidetodoc.com/medium-frequency-ground-penetrating-radar-gpr-ground-penetrating/ (accessed November 8, 2021).

[4]   N. Gucunski, F. Romero, S. Kruschwitz, R. Feldmann, H. Parvardeh, Comprehensive bridge deck deterioration mapping of nine bridges by nondestructive evaluation technologies., Iowa. Dept. of Transportation, 2011.

[5]   H.M. Jol, Ground Penetrating Radar Theory and Applications, elsevier, 2016. https://doi.org/10.1016/b978-0-444-53348-7.x0001-4.

[6]   R. Parrillo, R. Roberts, Bridge Deck Condition Assessment using Ground Penetrating Radar, 2006. http://citeseerx.ist.psu.edu/viewdoc/download?doi=10.1.1.159.3634&rep=rep1&type=pdf (accessed April 17, 2019).

[7]   N. Gucunski, A. Imani, F. Romero, S. Nazarian, D. Yuan, H. Wiggenhauser, P. Shokouhi, A. Taffe, D. Kutrubes, Nondestructive Testing to Identify Concrete Bridge Deck Deterioration, Transportation Research Board, Washington, D.C., 2012. https://doi.org/10.17226/22771.

[8]   C. Yuan, S. Li, H. Cai, V.R. Kamat, GPR Signature Detection and Decomposition for Mapping Buried Utilities with Complex Spatial Configuration, J. Comput. Civ. Eng. 32 (2018) 04018026. https://doi.org/10.1061/(asce)cp.1943-5487.0000764.

[9]   S. Perras, L. Bouchard, Fading characteristics of RF signals due to foliage in frequency bands from 2 to 60 GHz, Int. Symp. Wirel. Pers. Multimed. Commun. WPMC. 1 (2002) 267–271. https://doi.org/10.1109/WPMC.2002.1088174.

[10]   I.-S. Yoon, C.-H. Chang, Effect of chloride on electrical resistivity in carbonated and non-carbonated concrete, Appl. Sci. 10 (2020) 6272.

[11]   J.-Y. Rhee, J. Shim, S.-H. Kee, S.-Y. Lee, Different Characteristics of Radar Signal Attenuation Depending on Concrete Condition of Bare Bridge Deck, KSCE J. Civ. Eng. 24 (2020) 2049–2062. https://doi.org/10.1007/s12205-020-1840-1.

[12]   A.M. Alani, M. Aboutalebi, G. Kilic, Applications of ground penetrating radar (GPR) in bridge deck monitoring and assessment, J. Appl. Geophys. 97 (2013) 45–54. https://doi.org/10.1016/j.jappgeo.2013.04.009.

[13]   T. Chung, C.R. Carter, T. Masliwec, D.G. Manning, Impulse Radar Evaluation of Asphalt-Covered Bridge Decks, IEEE Trans. Aerosp. Electron. Syst. 28 (1992) 125–137. https://doi.org/10.1109/7.135439.

[14]   C.L. Barnes, J.-F. Trottier, Effectiveness of Ground Penetrating Radar in Predicting Deck Repair

Quantities, J. Infrastruct. Syst. 10 (2004) 69–76. https://doi.org/10.1061/(asce)1076-0342(2004)10:2(69).

[15]   K. Dinh, T. Zayed, S. Moufti, A. Shami, A. Jabri, M. Abouhamad, T. Dawood, Clustering-based threshold model for condition assessment of concrete bridge decks with ground-penetrating radar, Transp. Res. Rec. 2522 (2015) 81–89. https://doi.org/10.3141/2522-08.

[16]   M. Abouhamad, T. Dawood, A. Jabri, M. Alsharqawi, T. Zayed, Corrosiveness mapping of bridge decks using image-based analysis of GPR data, Autom. Constr. 80 (2017) 104–117. https://doi.org/10.1016/j.autcon.2017.03.004.

[17]   K. Dinh, N. Gucunski, J. Kim, T.H. Duong, Understanding depth-amplitude effects in assessment of GPR data from concrete bridge decks, NDT E Int. 83 (2016) 48–58. https://doi.org/10.1016/j.ndteint.2016.06.004.

[18]   K. Dinh, N. Gucunski, T.H. Duong, Migration-based automated rebar picking for condition assessment of concrete bridge decks with ground penetrating radar, NDT E Int. 98 (2018) 45–54. https://doi.org/10.1016/j.ndteint.2018.04.009.

[19]   S. Abu Dabous, S. Yaghi, S. Alkass, O. Moselhi, Concrete bridge deck condition assessment using IR Thermography and Ground Penetrating Radar technologies, Autom. Constr. 81 (2017) 340–354. https://doi.org/10.1016/j.autcon.2017.04.006.

[20]   A.A. Sultan, G.A. Washer, Reliability Analysis of Ground-Penetrating Radar for the Detection of Subsurface Delamination, J. Bridg. Eng. 23 (2018) 04017131. https://doi.org/10.1061/(ASCE)BE.1943-5592.0001182.

[21]   A. V. Varnavina, A.K. Khamzin, E. V. Torgashov, L.H. Sneed, B.T. Goodwin, N.L. Anderson, Data acquisition and processing parameters for concrete bridge deck condition assessment using ground-coupled ground penetrating radar: Some considerations, J. Appl. Geophys. 114 (2015) 123–133. https://doi.org/10.1016/j.jappgeo.2015.01.011.

[22]   C.L. Barnes, J.F. Trottier, D. Forgeron, Improved concrete bridge deck evaluation using GPR by accounting for signal depth-amplitude effects, NDT E Int. 41 (2008) 427–433. https://doi.org/10.1016/j.ndteint.2008.03.005.

[23]   A.M. Alani, M. Aboutalebi, G. Kilic, Applications of ground penetrating radar (GPR) in bridge deck monitoring and assessment, J. Appl. Geophys. 97 (2013) 45–54.

[24]   K. Dinh, T. Zayed, M. Asce, ; Francisco Romero, A. Tarussov, Method for Analyzing Time-Series GPR Data of Concrete Bridge Decks, (2014). https://doi.org/10.1061/(ASCE).

[25]   A. Benedetto, A three dimensional approach for tracking cracks in bridges using GPR, J. Appl. Geophys. 97 (2013) 37–44. https://doi.org/10.1016/j.jappgeo.2012.12.010.

[26]   M.I. Hasan, N. Yazdani, Ground penetrating radar utilization in exploring inadequate concrete covers in a new bridge deck, Case Stud. Constr. Mater. 1 (2014) 104–114. https://doi.org/10.1016/j.cscm.2014.04.003.

[27]   J. Hugenschmidt, Concrete bridge inspection with a mobile GPR system, Constr. Build. Mater. 16 (2002) 147–154. https://doi.org/10.1016/S0950-0618(02)00015-6.

[28]   J. Hugenschmidt, R. Mastrangelo, GPR inspection of concrete bridges, Cem. Concr. Compos. 28 (2006) 384–392.

[29]   A. V Varnavina, A.K. Khamzin, L.H. Sneed, E. V Torgashov, N.L. Anderson, N.H. Maerz, K.J. Boyko, Concrete bridge deck assessment: Relationship between GPR data and concrete removal depth measurements collected after hydrodemolition, Constr. Build. Mater. 99 (2015) 26–38.

[30]   A. V. Varnavina, L.H. Sneed, A.K. Khamzin, E. V. Torgashov, N.L. Anderson, An attempt to describe a relationship between concrete deterioration quantities and bridge deck condition assessment techniques, J. Appl. Geophys. 142 (2017) 38–48. https://doi.org/10.1016/j.jappgeo.2017.05.009.

[31]   X. Wei, Y. Zhang, Autofocusing techniques for GPR data from RC bridge decks, IEEE J. Sel. Top. Appl. Earth Obs. Remote Sens. 7 (2014) 4860–4868. https://doi.org/10.1109/JSTARS.2014.2321710.

[32]   A.L. Salomon, C.D. Moen, Structural design guidelines for concrete bridge decks reinforced with corrosion-resistant reinforcing bars., Virginia. Dept. of Transportation, 2014.

[33]   D.C.B. Cintra, P.M.B. Manhães, F.M.C.P. Fernandes, D.M. Roehl, J.T. ARARUNA, E.S. SÁNCHEZ, Evaluation of the GPR (1.2 GHz) technique in the characterization of masonry shells of the Theatro Municipal do Rio de Janeiro, Rev. IBRACON Estruturas e Mater. 13 (2020) 274–297.

[34]   GSSI, SIR 4000 Manual, Nashua, NH, 2017.

[35]   U. Boniger, J. Tronicke, On the potential of kinematic GPR surveying using a self-tracking total station: Evaluating system crosstalk and latency, IEEE Trans. Geosci. Remote Sens. 48 (2010) 3792–3798.

[36]   C. Warren, A. Giannopoulos, I. Giannakis, gprMax: Open source software to simulate electromagnetic wave propagation for Ground Penetrating Radar, Comput. Phys. Commun. 209 (2016) 163–170. https://doi.org/10.1016/j.cpc.2016.08.020.

[37]   D. Goodman, S. Piro, GPR remote sensing in archaeology, Springer Berlin Heidelberg, Berlin, Heidelberg, 2013. https://doi.org/10.1007/978-3-642-31857-3.

[38]   K.M. Belli, R.A. Birken, R.A. Vilbig, S.J. Wadia-Fascetti, Simulated GPR investigation of deterioration in reinforced concrete bridge decks, in: 26th Symp. Appl. Geophys. to Eng. Environ. Probl. 2013, SAGEEP 2013, 2013: pp. 277–286. https://doi.org/10.4133/sageep2013-099.1.

[39]   M. Pal, Random forest classifier for remote sensing classification, Int. J. Remote Sens. 26 (2005) 217–222.

[40]   N. Dalal, B. Triggs, Histograms of oriented gradients for human detection, in: Proc. - 2005 IEEE Comput. Soc. Conf. Comput. Vis. Pattern Recognition, CVPR 2005, 2005: pp. 886–893. https://doi.org/10.1109/CVPR.2005.177.

[41]   L. Breiman, Random Forests, Mach. Learn. 2001 451. 45 (2001) 5–32. https://doi.org/10.1023/A:1010933404324.

[42]   S.T. Buckland, A.C. Davison, D. V. Hinkley, Bootstrap Methods and Their Application, Cambridge university press, 1998. https://doi.org/10.2307/3109789.

[43]   P. Kaur, K.J. Dana, F.A. Romero, N. Gucunski, Automated GPR Rebar Analysis for Robotic Bridge Deck Evaluation, IEEE Trans. Cybern. 46 (2016) 2265–2276. https://doi.org/10.1109/TCYB.2015.2474747.

[44] A. Neubeck, L. Van Gool, Efficient non-maximum suppression, in: 18th Int. Conf. Pattern Recognit., IEEE, 2006: pp. 850–855.

[45] C. Maas, J. Schmalzl, Using pattern recognition to automatically localize reflection hyperbolas in data from ground penetrating radar, Comput. Geosci. 58 (2013) 116–125. https://doi.org/10.1016/j.cageo.2013.04.012.

[46] Z.W. Wang, M. Zhou, G.G. Slabaugh, J. Zhai, T. Fang, Automatic detection of bridge deck condition from ground penetrating radar images, IEEE Trans. Autom. Sci. Eng. 8 (2011) 633–640. https://doi.org/10.1109/TASE.2010.2092428.

[47] P. Virtanen, R. Gommers, T.E. Oliphant, M. Haberland, T. Reddy, D. Cournapeau, E. Burovski, P. Peterson, W. Weckesser, J. Bright, SciPy 1.0: fundamental algorithms for scientific computing in Python, Nat. Methods. 17 (2020) 261–272.

[48] M.A. Fischler, R.C. Bolles, Random sample consensus: a paradigm for model fitting with applications to image analysis and automated cartography, Commun. ACM. 24 (1981) 381–395.

[49] H. Sun, S. Pashoutani, J. Zhu, Nondestructive evaluation of concrete bridge decks with automated acoustic scanning system and ground penetrating radar, Sensors (Switzerland). 18 (2018) 1955. https://doi.org/10.3390/s18061955.

[50] C. Leys, C. Ley, O. Klein, P. Bernard, L. Licata, Detecting outliers: Do not use standard deviation around the mean, use absolute deviation around the median, J. Exp. Soc. Psychol. 49 (2013) 764–766.

[51] C.B. Barber, D.P. Dobkin, H. Huhdanpaa, The Quickhull Algorithm for Convex Hulls, ACM Trans. Math. Softw. 22 (1996) 469–483. https://doi.org/10.1145/235815.235821.